Anticancer effects of sanguinarine in triple-negative breast cancer cells via apoptosis induction and cell cycle arrest

Samia S. Messeha
Florida A&M University
Sophie Noel
Florida A&M University
Najla O. Zarmouh
Libyan Ministry of Technical & Vocational Education
Tracy Womble
Florida A&M University
Karam Soliman (karam.soliman@famu.edu)
Florida A&M University

Article

Keywords: sanguinarine, triple-negative breast cancer, MDA-MB-231, MDA-MB-468, cell cycle, apoptosis, mRNA, gene expression

Posted Date: May 9th, 2022

DOI: https://doi.org/10.21203/rs.3.rs-1602051/v1

Abstract

Patients with triple-negative breast cancer (TNBC) are typically treated with non-targeted chemotherapeutic agents, and the late disease stages are known to be resistant to chemotherapy. Therefore, it is necessary to develop novel therapeutic agents that are safer and more effective for enhancing the outcomes of chemotherapeutic agents. The natural alkaloid sanguinarine (SANG) is a quaternary benzophenanthridine alkaloid that has demonstrated synergistic therapeutic effects when combined with various chemotherapeutic drugs. SANG can also induce cell cycle arrest and trigger apoptosis in various cancer cells. Therefore, in this study, we investigated the molecular mechanism underlying SANG activity in MDA-MB-231 and MDA-MB-468 cells, as two genetically different models of TNBC. SANG decreased the viability of both cell lines, but MDA-MB-468 cells were more sensitive to SANG than MDA-MB-231 cells. SANG affected cell cycle progression in both cell lines. Further, S-phase cell cycle arrest-mediated apoptosis was found to be the primary contributor to cell growth inhibition in MDA-MB-231 cells. SANG-treated TNBC cells showed significantly upregulated mRNA expression of 18 genes associated with apoptosis, including eight members of the TNF receptor superfamily (*TNFRSF*), three members of the BCL2 family, and two members of the caspase (*CASP*) family in MDA-MB-468 cells; in MDA-MB-231 cells, two members of the TNF superfamily and four members of the BCL2 family were affected. In conclusion, these results indicate that SANG shows markedly different anticancer effects and apoptosis-related gene expression changes in the two cell lines. Thus, SANG demonstrates potent anticancer effects in TNBC cell lines, suggesting its potential as a single or adjunct therapeutic agent against TNBC.

1. Introduction

In the United States, breast cancer (BC) is the most common malignancy and the second leading cause of death among women aged 20–59 years [1]. Gene expression is controlled by molecular signal transduction, and alterations in transcriptional settings are characteristic of cancer cells [2]. BC is a heterogeneous cancer type categorized based on its molecular features. Triple-negative breast cancer (TNBC) that affects approximately 15% of patients with BC [2]. However, the incidence of this subtype is two to three times higher in African American (AA) women than in other ethnic groups [3,4]. TNBC is the most aggressive BC, and has a poor outcome compared to other BC subtypes [3]. Based on immunohistochemical characteristics, TNBC cells lack the expression of estrogen receptor (ER), progesterone receptor (PR), and human epidermal growth factor receptor 2 (HER2) [3,5]. Currently, chemotherapy is the primary treatment for patients with TNBC. However, disease recurrence can manifest within the first two years with an aggressive metastatic pattern [6]. Hence, the continuous pursuit of novel agents is necessary and novel drugs with the potential to induce cell cycle arrest and apoptosis are being pursued for cancer therapy [7].

In cancer, the characteristic mechanism of tumors to overcome DNA damage is a high proliferation rate, boosted by rapid cell cycle progression [8]. The signaling pathways controlling these events affect cancer

cells significantly [9]. Indeed, retracting the cell cycle checkpoints preceding DNA repair can promote apoptotic signaling, leading to transcriptional suppression and cell death [10]. Apoptosis is a controlled process that maintains cellular homeostasis and is mediated by extrinsic (death receptor (DR)-mediated) and intrinsic (mitochondrial or BCL2-dependent) pathways. The nature of the stimulus is the main contributing factor leading to the activation of either or both apoptotic pathways [11-15]. The extrinsic apoptotic pathway is initiated upon binding of pro-apoptotic ligands, such as tumor necrosis factor-alpha (TNF-α), and FAS ligand with their respective transmembrane receptors, which activate proteases known as caspases, leading to cell death. Induction of the intrinsic apoptotic pathway occurs instantaneously with increasing mitochondrial membrane permeability and the release of different pro-apoptotic proteins, such as cytochrome c (Cyt-c) and apoptosis-inducing factor (AIF), which disrupts the balance between anti-apoptotic and pro-apoptotic proteins, leading to caspase-dependent and/or independent cell death [16,17]. Therefore, induction of cell cycle arrest and apoptosis has been considered a promising approach for treating BC [15,18,19]

Sanguinarine (SANG), a benzophenanthridine alkaloid derived from the rhizomes of *Sanguinaria canadensis* plants, has remarkable biological activity and anticancer potential [17]. The anticancer effect of SANG has been strongly linked with its ability to induce cell death via the extrinsic and intrinsic apoptotic pathways [17,20], as well as to induce DNA fragmentation [21-24]. SANG has been reported to induce apoptosis in prostate cancer [25-47] and BC cells [48-52]. SANG can also induce apoptosis via free radical initiation and mitochondrial dysfunction [31,32]. These mechanisms affect different proteins, including signal transducer and activator of transcription 3 (STAT3), p53, B-cell lymphoma 2 (BCL2) family members, caspases, inhibitor of apoptosis family (IAP), and extracellular signal-regulated kinase 1/2 (ERK1/2) [17,53]. In MDA-MB-231 TNBC cells, SANG has demonstrated apoptotic effects by upregulating apoptosis-mediated proteins (p27, Cyt-c, and truncated BH3 interacting domain death agonist (tBID)), while inhibiting others (cyclin D1, STAT3, x-link IAP; XIAP, cIAP-1, cIAP-2, and BCL2; CASP8 and FADD-like apoptosis regulator; and *c-FLIP*/*CFLAR*) [49,51-54].

Resistance to chemotherapy-induced cytotoxicity is a major challenge in cancer therapy [17]. Therefore, drug combinations are crucial to achieve significant synergistic therapeutic effects [55]. In various chemotherapeutic drug-resistant cancer cells, SANG has been shown to enhance the anticancer effects of multiple drugs [56,57], including doxorubicin [58] and paclitaxel [27]. In MDA-MB-231 BC cells, SANG can synergize with TNF-related apoptosis-inducing ligand (TRAIL)-linked apoptosis [52]. Further, the combination of SANG with a sub-lethal dose of digitonin induces an increased cytotoxic effect in MCF-7 BC cells [59].

Although the anti-apoptotic effects of SANG in the MDA-MB-231 TNBC cell model have been reported, its effects on MDA-MB-468 cells, a phenotypically distinct TNBC cell line, have not yet been studied. Therefore, this comparative study aimed to determine the link between phenotype-related gene expression and sensitivity to SANG in these two TNBC models. We also analyzed the impact of SANG on genes

mediating apoptosis in both models under identical experimental settings using a human apoptosis gene expression array.

2. Materials And Methods

2.1 Cell culture and media

The human TNBC cell lines MDA-MB-231 (ATCC® HTB-26™) and MDA-MB-468 (ATCC® HTB-132™) were purchased from ATCC (Manassas, VA, USA). MDA-MB-231 and MDA-MB-468 cells were derived from Caucasian American (CA) and African American (AA) individuals, respectively. Cell culture media and supplements were purchased from ATCC (VWR International, Radnor, PA, USA), Santa Cruz Biotechnology, Inc. (Dallas, TX, USA), and Thermo Fisher Scientific (Waltham, MA, USA). Both cell lines were grown as monolayers in tissue culture flasks and maintained at 37°C with 5% CO_2 in a humidified environment. The TNBC cell lines were cultured in Dulbecco's modified Eagle's medium (DMEM) containing 4 mM L-glutamine, supplemented with 10% heat-inactivated fetal bovine serum (FBS), 100 U/ml penicillin, and 0.1 mg/ml streptomycin (1% P-S). The media were changed as required after washing the cells with Dulbecco's phosphate-buffered saline (DPBS), and the cells were sub-cultured using phenol-free trypsin/ethylenediaminetetraacetic acid (EDTA, 0.25%). Experimental media supplemented with 2.5% heat inactivated FBS were used for all assays.

2.2. Cell viability assay

The effect of SANG on the viability MDA-MB-231 and MDA-MB-468 cell viability was determined using Alamar Blue® (AB®, Sigma-Aldrich, St. Louis, MO, USA) as previously described [60]. The alkaloid compound sanguinarine chloride hydrate ≥ 98% (HPLC) was purchased from Sigma-Aldrich and reconstituted at a concentration of 15 mM in dimethyl sulfoxide (DMSO, ATCC), aliquoted, and stored at -20°C for later use. TNBC cells were seeded in quintuplicate at 5×10^4 cells/100 µL/well in 96-well plates and incubated overnight at 37°C in a humidified atmosphere with 5% CO_2. TNBC cells were then treated with DMSO (≤ 0.1%) or graded concentrations of SANG (0–5 µM). After 24 h of incubation, 20 µL of AB® resazurin solution (0.5 mg/ml in sterile phenol red-free HBSS) was added to each well followed by further incubation for 4 h at 37°C. The fluorescence intensity, indicating the reduction of resazurin by metabolically active TNBC cells, was measured at an excitation/emission wavelength of 530/590 nm using a Synergy HTX Multi-Mode microplate reader (BioTek Instruments, Inc., Winooski, VT, USA). The data obtained from the cell viability analysis were presented as the average of three independent experiments.

2.3. Cell proliferation assay

The effect of SANG on cell proliferation was evaluated in TNBC cell lines, MDA-MB-231 and MDA-MB-468, using the same protocol as the cell viability assay with essential modifications [60]. Briefly, the experiment was initiated with seeding 1×10^4 cells/100 µL/well. The cells were then treated for 48–96 h

with SANG at concentrations ranging from 0–2.0 μM. The control wells were treated with DMSO at the highest concentrations (< 0.1%).

2.4. Flow cytometry assays

2.4.1. Cell cycle analysis

Cell cycle evaluation of SANG-treated TNBC cells was performed using a previously described protocol [60]. Briefly, cells seeded at 1.5×10^6 cells/4 ml/T25 cell culture flask were incubated overnight under the same incubation conditions. SANG was added in another 2 ml at four concentrations (0–1.5 μM) to each cell line. Cells corresponding to the control wells were treated with DMSO at the highest concentration of SANG (< 0.1%). After 24 h, cells from each treatment group were harvested, centrifuged at 1,000 rpm for 5 min, washed in DPBS, fixed in cold 70% ethanol, and kept in the refrigerator for at least four hours. The suspended cells were gently vortexed, pelleted, and washed twice with Dulbecco's phosphate-buffered saline. Finally, the cells were resuspended in 200 μl 1X propidium iodide (PI) with RNase staining solution (Abcam, Cambridge, MA, USA) and incubated for 30 min at 37°C in the dark. The cell distributions across the cell cycle were established using a FACSCalibur flow cytometer (BD Biosciences, San Jose, CA, USA). The data presented were generated from three independent analyses for each cell line.

2.4.2. Apoptosis assay

To establish the apoptotic effect of SANG in TNBC cells, we followed a previously described protocol [60] using the Annexin V-FITC (Ann FITC) Apoptosis Detection Kit Plus (Ray-Biotech, Norcross, GA, USA). Briefly, MDA-MB-231 and MDA-MB-468 cells were seeded at 5×10^5 cells/2 ml/well in 6-well plates and incubated overnight. The cells were treated for 24 h with optimized doses of SANG ranging from to 0–4.5 μM for MDA-MB-231 cells and 0–4.0 μM for MDA-MB-468 cells. The corresponding control wells were exposed to DMSO at a concentration equivalent to that in the highest tested dose (< 0.1%). After the pre-designated experimental period, cells from each well were collected, centrifuged, and washed in DPBS. In another set of tubes, cell pellets were resuspended in 500 μL of 1X Annexin V binding buffer, and sequentially labeled for 10 min with 5 μL each of Ann FITC and PI. A flow cytometer was used to analyze apoptosis in 1×10^4 events/sample. Unstained samples indicated live cells. Annexin V-stained cells were considered apoptotic, whereas cells in the late apoptotic or necrotic phases were positive for both Annexin-V and PI. Cell-Quest software was used to determine the percentage of apoptotic and necrotic cells in each treatment.

2.5. Gene expression analyses

2.5.1. Treatment of TNBC cells

Two T75 flasks seeded with 10×10^6 cells/10 ml for each line were designated as either DMSO-or SANG-treated cells. Each cell line was treated with the compound at the specified concentration corresponding to its IC_{50} value obtained from the viability study (3.5 μM in MDA-MB-231 cells and 2.6 μM in MDA-MB-

468 cells) [61, 62], following overnight incubation. Control cells were treated with DMSO at a concentration equivalent to that in the tested SANG concentration (≤ 0.1% DMSO). After 24 h of treatment with or without SANG, the cells from each flask were collected in a fresh tube, pelleted, washed with DPBS, and stored at -80°C for later use.

2.5.2. RNA extraction

According to the manufacturer's guidelines, RNA was extracted from previously frozen cell samples in 1 ml of TRIzol reagent (Thermo Fisher Scientific, Inc., Waltham, MA, USA) and homogenized briefly for 20 s. Then, 0.2 ml of chloroform (Sigma-Aldrich) was added to each vial for phase separation, vortexed, and incubated for 3 min at room temperature. All samples were then centrifuged for 15 min at 10,000 × *g* and 8°C. The RNA-rich upper layer was transferred to a fresh tube with 0.5 ml of 2-propanol to precipitate the RNA. The obtained pellets were washed with 75% ethanol, air-dried for 10 min, and reconstituted in 50 µL nuclease-free water.

2.5.3. Complementary DNA (cDNA) synthesis

The purity and concentration of RNA from each sample were determined using a NanoDrop spectrophotometer (NanoDrop Technologies, Thermo Fisher Scientific, Inc.). Next, 5 µg/ml of RNA was incubated with a 1X DNase cocktail using a DNA-free kit ((Thermo Fisher Scientific) for 30 min at 37°C. The reaction was terminated by adding a DNase inactivator. All samples were then centrifuged at 9,000 rpm for 3 min to precipitate the unwanted cellular DNA and the DNA-free supernatant was collected for cDNA synthesis by reverse transcription (RT). cDNA was generated using the iScript™ cDNA Synthesis kit (Bio-Rad Laboratories, Hercules, CA, USA). Each well of 96-well PCR plates was loaded with 5 µL of DNA-free RNA, 9 µL of nuclease-free water, and 6 µL of advanced reaction mix reverse transcriptase cocktail. The RT reaction was performed as follows: RT for 20 min at 46°C and RT inactivation for 1 min at 95°C. The cDNA obtained from each sample was stored at -80°C for the PCR assay.

2.5.4. Quantitative reverse transcriptionpolymerase chain reaction (qRTPCR) apoptosis array

A 96-well human apoptosis array (SAB Target List, cat #10034106, Bio-Rad) was loaded with 10 µL of cDNA (2.3 ng) and Sso Advanced™ Universal SYBR® Green Supermix (Bio-Rad) for a total volume of 20 µL/well. The plate was briefly shaken for 5 min and centrifuged at 1,000 × g; fluorescence quantification was performed using the Bio-Rad CFX96 Real-Time System (Bio-Rad). cDNA was amplified through 39 cycles of denaturation beginning with 30 s of activation at 95°C, 10 s of denaturation at 95°C, and 20 s of annealing at 60°C. The final extension step was completed at 65°C for 31 s. The qRT-PCR data were confirmed for each cell line using at least three independent experiments.

2.6. Statistical analysis.

The data obtained from this study were analyzed using GraphPad Prism 6.2 software (GraphPad Software, Inc., San Diego, CA, USA). Data are expressed as mean ± SEM from three biological replicates. The IC_{50} values were calculated using a nonlinear regression model of log (inhibitor) *vs.* the normalized

response-variable slope in the software with the R^2 best fit and the lowest 95% confidence interval. An Excel spreadsheet was used to calculate the IC50 ± SEM average of biological replicates. Cell cycle distribution and apoptosis data were analyzed using CellQuest software (BD Biosciences, San Jose, CA, USA). CFX 3.1 Manager software (Bio-Rad) was used to quantify gene expression in the apoptosis arrays. The significance of differences was determined using analysis of variance (ANOVA) followed by Bonferroni's multiple comparison test. Unpaired Student's t-test was used to analyze two datasets. One-way analysis of variance was used to compare more than two groups. Differences were considered significant at $P < 0.05$ (as mentioned in the figures and legends).

3. Results

3.1 Sanguinarine cytotoxic effects

The cytotoxic effects of SANG in MDA-MB-231 and MDA-MB-468 TNBC models were examined using AB® assays to detect metabolically active cells. Figure 1 shows the dose-dependent inhibition of cell viability in both cells following 24 h exposure to SANG. The IC_{50} values indicate that MDA-MB-468 cells are more sensitive to SANG (IC_{50} = 2.60 µM) than MDA-MB-231 cells (IC50 = 3.56 µM). MDA-MB-468 cells showed a highly significant decrease of 20% ($P < 0.0001$) in cell viability at all tested concentrations, starting with 1µM µM SANG.

The same effect was noted at 2.5 µM in MDA-MB-231 cells. This finding confirmed a 2.5-fold greater sensitivity in MDA-MB-468 cells than in MDA-MB-231 cells.

3.2. Sanguinarine inhibits the proliferation of triple-negative breast cancer cells

The antiproliferative effect of SANG was evaluated in both MDA-MB-231 and MDA-MB-468 TNBC cells using the AB® assay to determine the effect of the compound on the cellular metabolic activities. In both cell lines, SANG inhibited proliferation in a dose- and time-dependent manner compared with that in DMSO-treated control cells (Fig. 2a and b). Inhibition of cell proliferation was validated by the decrease in IC_{50} values at different periods of exposure (48–96 h). The effect of SANG at different exposure periods *vs*. the control indicated a similar response in both cell lines, with MDA-MB-468 being more sensitive. Indeed, a highly significant reduction ($P < 0.0001$) in cell proliferation was found with 0.25 µM in MDA-MB-468 cells and with 0.75 µM in MDA-MB-231 cells. Furthermore, a highly significant difference ($P < 0.0001$) was also observed between different exposure periods, except for a non-significant difference between the 48 h *vs*. 72 h treatment periods in MDA-MB-468 cells (NS; Fig. 2b).

3.3. Sanguinarine affects cell cycle progression in triple-negative breast cancer cells

To test the hypothesis that cell cycle blockade mediates SANG-induced cytotoxic and antiproliferative effects, we performed flow cytometric analysis using the fluorescent probe PI. Following 24 h exposure, the response of the SANG-treated cells was compared with that that of DMSO-control cells (Fig. 3a and b). The figures showed only a slight change in cell distribution

among the three phases of the cell cycle in the MDA-MB-468 cells (Fig. 3b). In contrast, significant dose-dependent changes ($P < 0.05$–$P < 0.0001$, Fig. 3a) were observed in the SANG-treated MDA-MB-231 cells. At the highest tested concentration of 1.5 μM, the DNA histogram exhibited a sub-G1 phase (~ 25%) in MDA-MB-231 cells (Fig. 3a), which suggested the presence of dead cells, but this was not detected in MDA-MB-468 cells (Fig. 3b). A significant decrease in the G0/G1 phase (20%; $P < 0.05$–$P < 0.001$) was observed in MDA-MB-231 cells compared with only a minor reduction (~ 6%; $P < 0.01$–$P < 0.001$) in MDA-MB-468 cells. Consequently, MDA-MB-231 cells arrested at the S phase and G2/M phase increased by approximately 15% and 5%, respectively ($P < 0.001$-$P < 0.0001$; Fig. 3a). Meanwhile, lower concentrations of SANG (0.5 and 1.0 μM) induced less than 10% increase in the S-phase, accompanied with a minor but significant accumulation ($P < 0.01$, Fig. 3b) in the G2/M phase of up to 7%, at 1.5 μM SANG. Thus, these data implicate cell cycle arrest in the SANG-induced antiproliferative effects observed in MDA-MB-231 cells. However, in MDA-MB-468 cells, this is not the leading mechanism, and other mechanisms may be involved.

3.4. Sanguinarine triggers apoptosis in triple-negative breast cancer cells

Flow cytometric analysis was performed to determine whether apoptosis was involved in the reduced in cell viability and proliferation rate by SANG. For this assay, TNBC cells were treated with SANG at various doses (2.5–4.5 μM in MDA-MB-231 cells and 1–4 μM in MDA-MB-468 cells). A significant increase in apoptotic cells was observed in SAN-treated cells compared to the control ($P < 0.001$–$P < 0.0001$; Fig. 4a and b). Notably, a slow rise in apoptosis across the tested concentrations was found from 3.0–4.5 μM SANG in MDA-MB-231 cells and 2.0–4.0 μM SANG in MDA-MB-468 cells. The AA model (MDA-MB-468) cells were approximately 3-fold more sensitive to SANG than MDA-MB-231 cells. At the lowest tested concentration (2.5 μM), SANG induced apoptosis in 30% of the treated MDA-MB-231 cells compared with the control (Fig. 4a), whereas 80% of the analyzed MDA-MB-468 cells were in the apoptotic phase following exposure to 2.0 μM SANG (Fig. 4b). Notably, at 4 μM of SANG, a higher percentage of necrotic cells was detected in MDA-MB-231 cells than in MDA-MB-468 cells (27% *vs*.8%, respectively), indicating the tendency of CA TNBC cells to undergo necrosis rather than apoptosis. Overall, the data suggest that apoptosis is a leading mechanism that mediates cell death in SANG-treated MDA-MB-468 cells.

3.5. Gene expression profile in sanguinarine-treated triple-negative breast cancer cells

The mechanism underlying the profound apoptotic effects in SANG-treated TNBC cells was further investigated using qRT-PCR. Following a previously described protocol [61,62], cells were treated for 24 h

with a specific dose of SANG equivalent to their IC_{50} values (3.5 μM for MDA-MB-231 cells and 2.6 μM for MDA-MB-468 cells; Fig. 1). An overview of the normalized apoptosis-related gene expression provided insight into the impact of SANG on various genes that regulate the apoptotic pathway (Fig. 5a and b). In the figure, the red dots indicate the upregulated genes in both cell lines. The green-colored dots representing the downregulated genes were observed only in MDA-MB-231 cells (Fig. 5a). The black dots in the middle panel indicate the range of unchanged gene expression in both cell line

Table I. Fold-change of mRNA gene expressions after 24h exposure to the alkaloid compound sanguinarine (SANG) at the corresponding IC_{50} s of 3.5 μM in MDA-MB-231 and 2.6 μM in MDA-MB-468 TNBC cells.

Control vs. treated MDA-MB-231 cells			**Control vs. treated MDA-MB-468 cells**		
Target gene	Fold (+/-)	p-value	Target gene	Fold (+)	p-value
LTA	+ 15.0	0.0122	*TNFRSF11B*	+ 4.41	0.0317
BAG3	+ 9.22	0.0114	*TNFRSF25*	+ 3.30	0.0023
BCL2L11	+ 4.67	0.0404	*HRK*	+ 3.21	0.0289
GADD45A	+ 4.17	0.0324	*BCL2L11*	+ 3.17	0.0047
BCL2A1	+ 3.65	0.0007	*TNFRSF10B*	+ 2.80	0.0070
LTBR	− 11.0	0.0227	*DFFA*	+ 2.57	0.0082
TP53	− 3.74	0.0196	*NOD1*	+ 2.56	0.0272
AKT1	− 3.35	0.0126	*TNFRSF10A*	+ 2.45	0.0015
CASP6	− 3.23	0.0031	*TNFRSF21*	+ 2.42	0.0091
BCL2L1	− 3.13	0.0028	*BIRC3*	+ 2.39	0.0047
GUSB	− 3.10	0.0187	*BAX*	+ 2.28	0.0008
BIRC5	− 1.85	0.0152	*DAPK1*	+ 2.22	0.0112
			CFLAR	+ 2.20	0.0054
			CASP10	+ 2.14	0.0105
			FADD	+ 2.13	0.0141
			TRADD	+ 1.96	0.0002
			TRAF2	+ 1.95	0.0114
			CASP1	+ 1.85	0.0384

MDA-MB-231 cells (left panel) showed mixed alterations in their mRNAs. The upregulated mRNAs: lymphotoxin alpha (*LTA*), BCL2-associated athanogene 3 (*BAG3*), BCL2 like protein 11 (*BCL2L11*), the growth arrest and DNA damage-inducible 45 alpha (*GADD45A*), and BCL2-related protein A1 (*BCL2A1*) and the repressed mRNAs, including lymphotoxin beta receptor cells, (*LTBR*), tumor protein p53 (*TP53*), BCL2 like protein 1 (*BCL2L1*), AKT serine/threonine kinase 1 (*AKT1*), *CASP6*, glucuronidase beta (*GUSB*), and baculoviral inhibitor of apoptosis family (IAP) repeat-containing 5 (*BIRC5*). In contrast, MDA-MB-468 cells gene expression analysis (right panel), showed only a significant upregulation in the mRNA of 18 genes, including TNF (tumor necrosis factor) receptor superfamily (*TNFRSF*) *11B* and *25*, harakiri BCL2 Interacting Protein (*HRK*), B-cell lymphoma 2 (BCL2) Like protein 11 (*BCL2L11*), *TNFRSF10B*, deoxyribonucleic acid (DNA) fragmentation factor subunit alpha (*DFFA*), nucleotide-binding oligomerization domain-containing protein 1 (*NOD1*), T*NFRSF10A / 21*, baculoviral (IAP) repeat-containing 3 (*BIRC3*), BCL2 associated X-protein (*BAX*), death-associated protein kinase 1 (*DAPK1*), CASP8 and FADD-like apoptosis regulator (*CFLAR*),), caspase (*CASP)10*, FAS-associated via death domain (*FADD*), TNFRSF1A associated via death domain (*TRADD*), TNF receptor associated factor 2 (*TRAF2*), and *CASP1*.

Several upregulated genes with significant roles in apoptosis were identified in MDA-MB-468 cells. This finding supports our previous flow cytometry data that indicate apoptosis as the leading mechanism activated by SANG to inhibit cell proliferation in this AA model. Indeed, after 24 h of exposure to 2.6 μM SANG, a total of 18 genes were significantly upregulated in the MDA-MB-468 cell model ($P < 0.05$–$P < 0.001$) with a 1.85-4.41-fold increase in their transcriptomic levels (Fig. 6a-d and Table 1). These augmented genes belonged to different protein families, as shown in Fig. 6. Eight members of the tumor necrosis factor (TNF) receptor superfamily (*TNFRSF*) were identified, including *TNFRSF11B* with the highest fold increase (+ 4.41), *TNFRSF25*, *TNFRSF10B/A*, *TNFRSF21*, FAS-associated via death domain (*FADD*), TNFRSF1A associated via death domain (*TRADD*), and TNF receptor-associated factor 2 (*TRAF2*) (Fig. 6a). Further, two members of the caspase (*CASP*) family, *CASP1* and *10* were upregulated in MDA-MB-468 cells (Fig. 6b), in addition to three members of the BCL2 family: BCL2 like protein 11 (*BCL2L11*), harakiri BCL2 interacting protein (*HRK*), and BCL2 associated X-protein (*BAX*) (Fig. 6c). More than two-fold increase was observed in five other genes, including the deoxyribonucleic acid (DNA) fragmentation factor subunit alpha (*DFFA*), baculoviral IAP repeat-containing 3 (*BIRC3*), nucleotide-binding oligomerization domain-containing protein 1 (*NOD1*), *CFLAR*, and death-associated protein kinase 1 (*DAPK1*) (Fig. 6d).

In contrast, the response of MDA-MB-231 cells to the compound was different. Fewer apoptosis-related genes were activated (Fig. 7a and b), with a significantly higher fold increase than in MDA-MB-468 cells. When exposed to 3.5 μM of SANG, the mRNA of five genes was remarkably augmented by 3.65–15.0-fold (Fig. 7a). Lymphotoxin alpha (*LTA*) was the most abundant gene (15-fold), followed by BCL2-associated athanogene 3 (*BAG3*), *BCL2L11*, growth arrest and DNA damage-inducible 45 alpha (*GADD45A*), and BCL2-related protein A1 (*BCL2A1*). *BCL2L11* was the only commonly upregulated gene in both cell models, but its upregulation was higher in MDA-MB-231 cells than in MDA-MB-468 cells (4.67 *vs*. 3.17-fold).

In contrast to MDA-MB-468 cells, the other seven genes were significantly downregulated in MDA-MB-231 cells (Fig. 7b), with lymphotoxin beta receptor cells (*LTBR*) being the most profoundly attenuated (-11.0-fold). A less than 4-fold decrease was observed in four genes, including the tumor protein p53 (*TP53*), AKT sereness/threonine kinase 1 (*AKT1*), *CASP6*, BCL2

like 1(*BCL2L1*), and glucuronidase beta (*GUSB*), in addition to the least repressed gene, baculoviral (IAP) repeat-containing 5 (*BIRC5*, -1.85-fold).

MDA-MB-231 cells (left panel) show mixed mRNA alterations. The upregulated mRNAs were lymphotoxin alpha (*LTA*), BCL2-associated athanogene 3 (*BAG3*), BCL2 like protein 11 (*BCL2L11*), growth arrest and DNA damage-inducible 45 alpha (*GADD45A*), and BCL2-related protein A1 (*BCL2A1*), and the repressed mRNAs were lymphotoxin beta receptor cells (*LTBR*), tumor protein p53 (*TP53*), BCL2 like protein 1 (*BCL2L1*), AKT serine/threonine kinase 1 (*AKT1*), *CASP6*, glucuronidase beta (*GUSB*), and baculoviral inhibitor of apoptosis family (IAP) repeat-containing 5 (*BIRC5*). In contrast, MDA-MB-468 cells (right panel) only showed significant upregulation of 18 genes, including TNF (tumor necrosis factor) receptor superfamily (*TNFRSF*) *11B, TNFRSF 25*, harakiri BCL2 Interacting Protein (*HRK*), B-cell lymphoma 2 (BCL2)-like protein 11 (*BCL2L11*), *TNFRSF10B*, deoxyribonucleic acid (DNA) fragmentation factor subunit alpha (*DFFA*), nucleotide-binding oligomerization domain-containing protein 1 (*NOD1*), TNFRSF10A /*21*, baculoviral (IAP) repeat-containing 3 (*BIRC3*), BCL2 associated X-protein (*BAX*), death-associated protein kinase 1 (*DAPK1*), CASP8, FADD-like apoptosis regulator (*CFLAR*), caspase (*CASP)10*, FAS-associated via death domain (*FADD*), TNFRSF1A associated via death domain (*TRADD*), TNF receptor-associated factor 2 (*TRAF2*), and *CASP1*.

4. Discussion

Naturally occurring compounds are promising therapeutic agents for managing different cancer types, including BC. The current study was designed to investigate the mechanism underlying the anticancer effect of the natural alkaloid SANG in two genetically different models of TNBC cells (Fig. 8). A panel of assays was performed to define the mechanism employed by SANG in these two cell lines. Consistent with other studies, our data strongly support the potency of 0–10 μM SANG in decreasing cell viability, proliferation rate, as well as cell cycle arrest and apoptosis induction in various cell models [21,25,26,30,39,42,54,63–67]. Remarkably, the obtained data indicate a higher cytotoxic potency in MDA-MB-468 cells than in MDA-MB-231 cells (Fig. 1). The compound showed substantial potential to decrease the proliferation rate (Fig. 2) in MDA-MB-468 cells compared to that in MDA-MB-231 cells. The difference in cell density is suggested as the main contributing factor leading to the obtained inhibition of cell proliferation meanwhile not affecting cell viability. Furthermore, SANG induced different patterns of cell cycle arrest in both cells, which manifested as high cell cycle interruption and a tendency to cause necrosis in MDA-MB-231 cells whereas MDA-MB-468 cells showed mild cell cycle arrest without necrosis. Indeed, further protein studies are required to interpret the effect of the compound on different phases. SANG can alter expression of various genes, orchestrating both intrinsic and extrinsic apoptosis pathways by employing different mechanisms in the two cell lines. The phenotypic differences in these

TNBC models could provide a rationale for the different mechanisms and potency outcomes that favor the MDA-MB-468 model. MDA-MB-231 and MDA-MB-468 cells are classified as TNBC cells; however, they have a different molecular profile. Generally, the incidence of TNBC is higher in AA compared with CA. The claudin-low MDA-MB-231 cells are triple-negative/basal-B mammary carcinoma, while the MDA-MB-468 cells are triple-negative/basal-A mammary carcinoma. Also, MDA-MB-231 cells are characterized by activating KRAS mutations and the protooncogene B-Raf and v-Raf murine sarcoma viral oncogene homolog B (BRAF). Compared with CA, mutation of KRAS and BRAF are not found in MDA-MB-468 cells [68]. The AA women exhibit epidermal growth factor receptor (EGFR) amplification and mutated phosphatase tensin homolog (PTEN), with higher somatic copy number alterations (CNA) segments and TP53 mutation, as well as a higher expression of the proliferative marker Ki-67 [69,70]. Meanwhile, a lower proportion of Phosphatidylinositol-4,5-Bisphosphate 3-Kinase Catalytic Subunit Alpha (PIK3CA) and DNA methylation levels is revealed in AA than in CA [71–74]. A less frequency of BRCA1, the tumor suppressor gene-mediating DNA repair, the mutation is found among AA women compared with its counterpart CA [75,76].

The ultimate goal of chemotherapeutic agents is to control cell cycle progression and enhance apoptosis [10]. Indeed, a close association between apoptosis and the cell cycle has been established [77]. Moreover, our cell cycle distribution analyses (Fig. 3) indicate a relatively discrete response in the two TNBC cell lines with respect to apoptosis (Fig. 4). In MDA-MB-468 cells, the minor response in the three phases indicates that cell cycle arrest was not the principal mechanism underlying the profound apoptotic effects in SANG-treated MDA-MB-468 cells. Therefore, we suggest the involvement of another apoptotic mechanism activated by SANG. In contrast, cell cycle arrest-mediated apoptosis was detected in MDA-MB-231 cells as evidenced in all phases, particularly the S-phase, and the most distinctive appearance of the sub-G1 peak, which is considered a biomarker for DNA damage-mediated apoptosis. Also, S-phase arrest is concord with a decreased G1/G0 and G2/M phases, reduced DNA synthesis, and it is the lead of reduced proliferation and cell viability [78,79].

In our study, transcript analysis of apoptosis-related genes in SANG-treated TNBC cells indicated that SANG has the potential to impact various genes by modulating both intrinsic and extrinsic pathways (Figs. 5–7). The mRNA expression profile showed a greater number of altered genes in MDA-MB-468 cells and confirmed the higher vulnerability of this cell model compared to MDA-MB-231 cells. The data showed that the 18 most significantly affected genes in MDA-MB-468 cells were upregulated. Meanwhile, SANG-treated MDA-MB-231 cells exhibited significant upregulation in the mRNA expression of five genes, and downregulation of seven genes, revealing the existence of two different mechanisms underlying the apoptotic pathway. Therefore, our results suggest a close association between cell genotype and gene expression changes in SANG-treated TNBC cells.

In the TNBC models investigated, SANG altered the expression of three caspase family members. In MDA-MB-468 cells, an almost 2-fold increase in the mRNA levels of *CASP1* and *CASP10* was observed. In contrast, only one caspase (*CASP6*) was affected in MDA-MB-231 cells and its expression was

significantly downregulated. Caspases are cysteine-related aspartate proteases that are expressed in immune and non-immune cells [80]. Under normal physiological conditions, caspases mediate both the intrinsic and extrinsic apoptosis pathways to sustain cellular homeostasis [12,81]. According to their cellular functions, caspases are classified as initiator, effector, or inflammatory caspases [82]. *CASP1* is a member of the inflammatory caspase family and has a unique function that is distinct from other apoptotic caspases [80]. In response to infection, CASP1 triggers pyroptosis, a type of cell death, as an innate immune mechanism that activates IL-1β and IL-18 [82]. Distinct from normal tissues, low *CASP1* expression has been detected in various types of cancer cells, including BC. Inhibiting *CASP1* expression was previously found to decrease apoptosis and promote proliferation, invasion, and progression in MDA-MB-231 cells [83]. In contrast, an elevated level of *CASP1* in fibroblasts is known to induce apoptosis and cell death [84]. In MCF7 BC cells, the initiator caspase *CASP10* sensitizes cells to TRAIL-induced apoptosis [85]. Previous reports have also suggested the anticipated role of *CASP1* with *CASP10* in inducing intrinsic apoptotic pathways by activating *BID* and increasing the mitochondrial release of Cyt-c [86–89]. In contrast, repression of *CASP6* in MDA-MB-231 cells indicated resistance to apoptosis (Fig. 7b). Indeed, *CASP6* is a downstream effector and executioner caspase that enhances apoptosis by activating various cellular proteins [90]. These findings support the role of *CASP1* and *CASP10* in promoting apoptosis in SANG-treated MDA-MB-468 cells and explain the weaker apoptotic response exhibited by MDA-MB-231 cells.

Three members of the BCL2 family were found to be upregulated in the TNBC cells in this study. The mRNA of *BCL2L11* was significantly increased in both TNBC cell models (Fig. 6c and 7a), whereas upregulated *HRK* and *BAX* were exclusive to MDA-MB-468 cells (Fig. 6c). The BCL2 family regulates the intrinsic apoptotic pathway through two main groups of proteins: pro- and anti-apoptotic proteins [13]. A balance between these two groups is essential for maintaining mitochondrial membrane integrity [91]. As a typical mechanism for resisting apoptosis, cancer cells upregulate anti-apoptotic proteins and downregulate pro-apoptotic proteins [92]. Previous studies using different cell lines have attributed the antiproliferative and proapoptotic effects of SANG to the imbalance between pro- and anti-apoptotic proteins [42].

In agreement with these findings, we suggest that SANG induces intrinsic apoptosis by altering the expression of various BcL-2 family members. One of the different mechanisms employed by cancer cells is the suppression of BCL2L11 (also known as *BIM*), which leads to tumor growth, metastasis, and drug resistance [93,94]. In contrast, forced upregulation of this gene in BC cells is known to alter the balance of BCL2 proteins to the apoptotic phenotype and the release of Cyt-c and Smac/DIABLO, which activate the caspase cascade [95]. Indeed, the pro-apoptotic gene *BCL2L11* contains BH3, a crucial factor in apoptosis induction [96]. Moreover, the dual function of *BCL2L11* in regulating autophagy and apoptosis may overcome the challenge of chemotherapeutic drug resistance [97,98]. Therefore, in treating BC subtypes, chemotherapeutic drugs such as doxorubicin and paclitaxel regulate *BCL2L11* expression and its signaling pathways as a potential mechanism apoptotic cell death [93,99]. Upregulated expression of *HRK* selectively abolishes the function of anti-apoptotic proteins and stimulates intrinsic mitochondrial

apoptosis [100,101]. The role of overexpressed *HRK* in inducing both intrinsic and extrinsic apoptosis pathways has been demonstrated in various cancer cell types, including BC cells [102–106], and is strongly linked to the existence of BH3 [96]. Furthermore, the ability of SANG to upregulate the effector pro-apoptotic protein *BAX* has been demonstrated in various cell models [31,33,34,37,42,107,108]. The upregulation of *BAX* mRNA has been demonstrated to antagonize the anti-apoptotic role of other BCL2 family members, leading to an increase in mitochondrial membrane permeability and cytochrome c release preceding caspase activation and apoptosis [109]. Arguably, we suggest that SANG induces intrinsic apoptosis by upregulating the expression of various proapoptotic members of the BCL2 family.

In MDA-MB-231 cells, two anti-apoptotic genes, *BCL2L1* and *BCL2A1*, were inversely altered (Fig. 7a and b), in addition to the significantly upregulated binding protein, *BAG* (Fig. 7a). Meanwhile, the mRNA of *BCL2L1* was downregulated, which is consistent with previously reported studies [40,42], and surprisingly, *BCL2A1* mRNA was significantly increased. In various cancer types, including TNBC, highly upregulated *BCL2A1* and *BCL2L1* (also known as *BCL-XL*) are closely associated with resistance to targeted agents and chemotherapeutic drugs [110–115]. Compared with normal breast tissues, upregulated *BCL2L1* levels are linked with BC initiation and progression, particularly at a higher grade of the disease, and are most likely associated with migration and metastasis [116–118]. Furthermore, various mechanisms are associated with apoptosis induction in BC, including *BCL2L1* pathway modulation [119], changing the *BAX*/*BCL2L1* ratio [120], and using *BCL2L1* antisense oligonucleotide [121]. Moreover, *BAG3* protein is considered a standard biomarker in specific cancer cells [122]. Overexpression of *BAG3* in various cancer types, including BC [123–127], inhibits apoptosis [128] while promoting proliferation [129] and chemotherapy resistance [130]. Thus, inhibiting *BAG3* expression is suggested as a promising strategy for cancer therapy [122]. Regulation of this gene in MDA-MB-231 cells could weaken the apoptotic effect of SANG in this model. Thus, we collectively suggest the implication of *BCL2A1* and *BAG3* upregulation in the relative resistance of MDA-MB-231 cells to SANG-induced intrinsic apoptosis compared with that in MDA-MB-468 cells.

Distinct from MDA-MB-231 cells, eight members of *TNFRSF* were significantly upregulated in SANG-treated MDA-MB-468 cells, including four death receptors (DRs): *TNFRSF25* (*DR3)*, *TNFRSF10A (DR4)*, *TNFRSF10B (DR5)*, and *TNFRSF21 (DR6)*, as well as *TNFRSF11B*, *FADD*, *TRADD*, and *TRAF2* (Fig. 6a). These death receptors on the cell surface transmit apoptotic signals once they bind to their specific death ligands [131]. Simultaneously, the advantage of inducing a selective apoptotic effect in cancer cells without harming healthy cells has led to the TRAIL-mediated apoptotic pathway being considered as a promising approach in cancer therapy [132]. Understanding the involvement of various TNFRSF family members in apoptosis has elucidated the prospects of modulating these proteins in cancer treatment [133]. Moreover, in BC, as well as in various other cancer cells, the adaptor molecules, *FADD* and *TRADD*, were previously found to interact with upregulated *TNFRSF25* and *TNFRSF10A/B* to enhance apoptosis by triggering TRAIL-mediated apoptosis [132,134–138]. These mechanisms induce various cellular signaling pathways, such as caspase activation, MAPK, and NF-κB [132,139–141]. Augmentation of all these *TNFRSF* genes in

MDA-MB-468 cells in our study strongly supports the previous findings. Therefore, we suggest that SANG induces the extrinsic apoptosis pathway via TRAIL-binding to its death receptor *TNFRSF10A/B* in SANG-treated MDA-MB-468 cells. In line with other findings in BC [142], upregulation of *FADD* mRNA in our study could also mediate the apoptotic effect observed in MDA-MB-468 cells. The ability of *TNFRSF21* to induce apoptosis [143], probably through the mitochondria-mediated intrinsic pathway and *BAX* interaction [144], suggest *TNFRSF21* and *BAX* upregulation as one of the mechanisms underlying apoptosis induction in SANG-treated MDA-MB-468 cells.

Our mRNA analysis also indicated upregulation of TRAF2 and *TNFRSF11B* mRNAs in MDA-MB-468 cells (Fig. 6a). Recent studies have demonstrated the involvement of dually functional *TRAF2* in both pro- and anti-apoptotic signals [145,146]. *TNFRSF11B* (also known as osteoprotegerin, OPG) is a well-known prognostic marker for BC [147,148]. Overexpression of this gene induces apoptosis resistance and enhances cancer cell viability, invasion, metastasis, and indicates poor prognosis [149,150]. Similarly, upregulated *TRAF2* induces apoptosis resistance by enhancing TNF-alpha-mediated activation of several pathways such as MAPK8/JNK and NF-□B. Hence, the transcriptomic upregulation of both *TNFRSF11B* and *TRAF2* could weaken the apoptotic potency of SANG in MDA-MB-468 cells. However, further investigation of the exact mechanism involving *TRAF2* in SANG-treated MDA-MB-468 cells is warranted.

In SANG-treated MDA-MB-468 cells, more than 2-fold upregulation was observed in the apoptosis-mediated gene, *CFLAR* (Fig. 6d). The role of this gene as an apoptosis inducer or inhibitor [151,152] is controversial, most likely because of its various isoforms. *CFLAR* has demonstrated the potency to inhibit the DR-induced apoptosis pathway, which inhibits *CASP8* stimulation [152–154]. Therefore, the role of *CFLAR* as an anti-apoptotic gene was anticipated in our study, mainly with unchanged expression of *CASP8* in SANG-treated MDA-MB-468 cells.

Two members of the IAP family, *BIRC3* (cellular IAP2) and *BIRC5* (survivin) [155,156], were inversely altered in SANG-treated TNBC cells (Fig. 6d and 7b). SANG treatment upregulated the expression of *BIRC3* mRNA in MDA-MB-468 cells and downregulated *BIRC5* levels in MDA-MB-231 cells. The IAP family is known to regulate the intrinsic and extrinsic apoptotic pathways, in addition to playing a minor role in the execution phase of apoptosis [156]. A recent study on invasive breast carcinomas negated the role of *BIRC3* in regulating any of these apoptotic pathways [155]. Two pro-oncogenic proteins [156], characterized by baculoviral IAP repeat (BIR) domains [155], are known to be involved in various signaling pathways that regulate cell viability, proliferation, differentiation, and apoptosis [157]. Elevated expression of these genes was previously detected in MDA-MB-231 and MDA-MB-468 TNBC cells, compared with that in normal breast cells [158–160] and was closely associated with resistance to apoptosis induction and chemotherapeutic efficacy [156,161–163]. Therefore, the obscure role of *BIRC3* upregulation in SANG-treated MDA-MB-468 cells require further investigation, even though *BIRC5* suppression in MDA-MB-231 cells could mediate apoptosis.

In MDA-MB-468 cells, only the pro-apoptotic gene *DAPK1* was significantly upregulated by SANG (Fig. 6d). *DAPK1* is involved in cell proliferation, autophagy, and immune response [164–166]. This gene is characterized by both the kinase domain and C-terminal death domain [167]. Low levels of *DAPK1* have been determined in various cancer types compared to control cells [168]. In addition, forced *DAPK1* upregulation through TNF-α or INF-γ [167] inhibits anti-apoptotic proteins [168] and ultimately induces apoptosis [169]. However, a recent study demonstrated a higher expression of *DAPK1* in BC cells, notably, in the most aggressive and metastatic TNBC cells with mutated p53, compared to that in healthy breast tissues [170,171]. Here, we suggest that *DAPK1* upregulation mediates apoptosis in MDA-MB-468 cells, particularly with unchanged anti-apoptotic genes.

Two other pro-apoptotic mRNAs, *DFFA* and *NOD1*, were found to be upregulated in SANG-treated MDA-MB-468 cells (Fig. 6d). These genes are crucial for caspase-dependent apoptotic pathways [172–174]. In cancer, *DFFA* (also known as *DFF45*, *DFF1*, or *ICAD*) acts as a substrate for caspase 3, triggering DNA fragmentation during apoptosis [172,173]. Reduced expression of *DFFA* has been measured in various cancer types as a part of an apoptosis-resistance mechanism for enhanced cancer progression [175]. Similarly, the protein *NOD1*-mediates apoptosis pathways by recruiting caspases through its characteristic domains [174] or directly through a RIPK2-dependent mechanism [176]. The abolished expression of *NOD1* in MCF-7 BC cells is closely associated with an increased estrogen-induced proliferation rate and failure to undergo *NOD1*-mediated apoptosis, as its overexpression significantly decreased cell proliferation [177–179]. Thus, our findings suggest *DFFA* and *NOD1* upregulation is one of the underlying mechanisms downstream of the apoptosis pathway in SANG-treated MDA-MB-468 cells.

In SANG-treated MDA-MB-231 cells, *LTBR* (also known as *TNFRSF3*) and its ligand *LTA*, were inversely and highly altered at -11-fold and + 15-fold, respectively (Fig. 7a, Table I). Analogous to other TNFSF members, these two proteins activate NF-κB signaling, mediating various cellular mechanisms including viability, proliferation, immune response, and apoptosis [180]. The dual role of *LTA* and *LTBR* in enhancing and suppressing tumor growth has been previously reported in an *in vivo* model [181–185]. Previous studies have demonstrated a crucial role of *LTA* transcriptomic upregulation in triggering apoptosis [186]. In contrast, other studies have suggested that repression of various signaling pathways leads to uncontrolled cancer cell proliferation [187]. This perplexing response of *LTA* and *LTBR* necessitates further investigation to identify the mechanism of LTA upregulation in MDA-MB-231 cells undergoing apoptosis.

The alkaloid compound SANG upregulates the expression of *GADD45A* by approximately 4-fold in MDA-MB-231 cells (Fig. 7a, Table I). In TNBC cells, low expression of *GADD45A*, together with p53 and DNA damage response genes, is linked with the lack of ER, PR, and HER2 expression [188]. This inducible stress gene regulates various cellular processes such as the cell cycle, DNA repair, and apoptosis [189] by activating multiple signaling pathways such as the c-Jun amino-terminal kinase (JNK), NF-κB, and p38 MAPK signaling pathways [190–194]. Hence, the impact of SANG in MDA-MB-231 cells (Figs. 2 and 4)

matches and agrees with the previously reported potential of *GADD45A* to induce anti-proliferative effects and S-phase cell cycle arrest [189].

Significant inhibition of *TP53* mRNA expression by SANG was detected only in MDA-MB-231 cells (Fig. 7b, Table I). Under normal conditions, *TP53* responds to various stresses by inducing different cellular processes such as cell cycle arrest, DNA repair, and apoptosis [195]. The main function of *TP53* is to prevent tumorigenesis and maintain genomic integrity [196]. However, mutated *TP53* loses its tumor-suppressor function and acquires oncogenic properties that enhance tumor progression [197]. Almost 80% of MDA-MB-231 and MDA-MB-468 TNBC patients are diagnosed with mutated *TP53*. This high level of mutated proteins is closely associated with poor prognosis and resistance to chemotherapy [198,199]. Although a previous study revealed an association between the antiproliferative and proapoptotic effects of SANG with the decreased levels of *TP53*[42], others highlighted the strong antiproliferative potential SANG regardless of *TP53* status [40]. Therefore, *TP53* repression could be a significant contributor to apoptosis in the MDA-MB-231 cell model.

Further, SANG showed the potential to attenuate the mRNA expression of *GUSB* and *AKT1* in MDA-MB-231 cells. Upregulated expression of *GUSB* has been implicated in an increased risk of cancer [200]. The chemopreventive effect of *GUSB* inhibitors has been validated by reduced cell proliferation and apoptosis induction in various cancer types, including BC [200–202]. Similarly, a tumor size reduction was found in *in vivo* models of BC upon combining *GUSB* inhibitors with the anticancer drug, irinotecan [203]. The multifunctional gene, *AKT1*, is a protein kinase B (AKT) isoform and the downstream effector of phosphatidylinositol 3-kinase (PI3K), which promotes cell growth by phosphorylating and controlling mammalian target of rapamycin (mTOR) signaling, as well as many targets [204–206]. Upregulation of *AKT1* in MDA-MB-231 cells and in patients with BC promotes proliferation and is closely associated with the aggressive nature of the disease [207–210]. The significance of targeting *AKT1* has been highlighted in other studies. For example, reduced AKT1 expression delays metastasis by inhibiting the Erb-B2 receptor tyrosine kinase 2 (ErbB2) pathway [209]. Silencing *AKT1* decreases lung colonization of TNBC cells mediated by apoptosis induction [211]. More importantly, knockdown of *AKT1* in MDA-MB-231 and MDA-MB-468 TNBC cells can enhance the expression of *BCL2L11*, a known promoter of apoptosis [211]. Therefore, our results strongly support these previous findings, as they suggest an association between *AKT1* attenuation and *BCL2L11* upregulation in SANG-treated MDA-MB-231 cells (Fig. 7a). Hence, inhibition of *AKT1* and *GUSB* expression in MDA-MB-231 cells [203] could be one of the key mechanistic factors involved in SANG-induced apoptosis.

5. Conclusions

The current study provides insights into the anticancer effects and the underlying molecular mechanism of the natural alkaloid SANG in two genetically different models of TNBC cells: the mesenchymal, MDA-MB-231, and the basal-like 1, MDA-MB-468 cells. Indeed, the variation in molecular profiles between the

two cell models including protein and gene expression, somatic DNA copy number alteration (CNA), somatic mutations, and DNA methylation patterns [74], could explain the different responses obtained in the treated cells. SANG significantly decreased the proliferation rate in both TNBC cell lines. In MDA-MB-468 cells, a profound apoptotic effect with very weak cell cycle arrest suggested the involvement of cell cycle arrest-independent apoptosis. Apoptosis-related gene arrays indicated that SANG alters the transcriptomic levels of various genes. Few studies have examined the clinical effect of SANG against cancer, even though herbal beverages with small doses of SANG have been used in folk medicine for treating many respiratory and heart diseases [212,213]. The current study highlights the need for further investigation in other TNBC models, *in vivo* and translational studies on SANG using the obtained data as the basis for developing molecularly targeted therapies to enhance the clinical outcomes of currently used chemotherapeutic agents in patients with TNBC.

Declarations

Author Contributions: Conceptualization, S.S.M. and K.F.A.S.; methodology, S.S.M.; validation, S.S.M., S.N., and T.W.; formal analysis, S.S.M.; investigation, S.S.M., S.N., and T.W.; resources, K.F.A.S.; data curation, S.S.M.; writing—original draft preparation, S.S.M.; writing—review and editing, S.S.M., N.O.Z., and K.F.A.S.; visualization, S.S.M.; supervision, S.S.M. and K.F.A.S.; project administration, S.S.M. and K.F.A.S.; funding acquisition, K.F.A.S. All authors have read and agreed to the published version of the manuscript.

Funding: This research was funded by a grant from the National Institute on Minority Health and Health Disparities (NIMHD) (U54 MD007582).

Acknowledgments: The authors are grateful for the assistance of Ramesh Badisa, College of Pharmacy and Pharmaceutical Science, Florida A&M University.

Institutional Review Board Statement: Not applicable.

Informed Consent Statement: Not applicable.

Data Availability Statement: All data generated or analyzed during this study are included in this published article.

Conflicts of Interest: The authors declare no conflicts of interest.

References

1. Siegel, R. L., Miller, K. D., Fuchs, H. E. & Jemal, A. Cancer Statistics, 2021. *CA Cancer J Clin* **71**, 7–33, doi:10.3322/caac.21654 (2021).
2. Perou, C. M. *et al.* Molecular portraits of human breast tumours. Nature **406**, 747–752, doi:10.1038/35021093 (2000).

3. Anders, C. K. & Carey, L. A. Biology, metastatic patterns, and treatment of patients with triple-negative breast cancer. *Clin Breast Cancer* **9 Suppl 2**, S73-81, doi:10.3816/CBC.2009.s.008 (2009).
4. Carey, L. A. *et al.* Race, breast cancer subtypes, and survival in the Carolina Breast Cancer Study. Jama **295**, 2492–2502, doi:10.1001/jama.295.21.2492 (2006).
5. Chavez, K. J., Garimella, S. V. & Lipkowitz, S. Triple negative breast cancer cell lines: one tool in the search for better treatment of triple negative breast cancer. Breast Dis **32**, 35–48, doi:10.3233/bd-2010-0307 (2010).
6. Barchiesi, G. *et al.* Early triple negative breast cancer: Are we getting better outcomes? A retrospective analysis from a single institution. Breast J **25**, 1225–1229, doi:10.1111/tbj.13437 (2019).
7. Malikova, J., Zdarilova, A. & Hlobilkova, A. Effects of sanguinarine and chelerythrine on the cell cycle and apoptosis. Biomed Pap Med Fac Univ Palacky Olomouc Czech Repub **150**, 5–12, doi:10.5507/bp.2006.001 (2006).
8. Vermeulen, K., Van Bockstaele, D. R. & Berneman, Z. N. The cell cycle: a review of regulation, deregulation and therapeutic targets in cancer. Cell proliferation **36**, 131–149, doi:10.1046/j.1365-2184.2003.00266.x (2003).
9. Wang, Z., Xie, Y. & Wang, H. Changes in survivin messenger RNA level during chemotherapy treatment in ovarian cancer cells. Cancer biology & therapy **4**, 716–719, doi:10.4161/cbt.4.7.1782 (2005).
10. Diaz-Moralli, S., Tarrado-Castellarnau, M., Miranda, A. & Cascante, M. Targeting cell cycle regulation in cancer therapy. Pharmacology & therapeutics **138**, 255–271, doi:10.1016/j.pharmthera.2013.01.011 (2013).
11. Galadari, S., Rahman, A., Pallichankandy, S., Galadari, A. & Thayyullathil, F. Role of ceramide in diabetes mellitus: evidence and mechanisms. Lipids Health Dis **12**, 98, doi:10.1186/1476-511x-12-98 (2013).
12. Galadari, S., Rahman, A., Pallichankandy, S. & Thayyullathil, F. Tumor suppressive functions of ceramide: evidence and mechanisms. Apoptosis **20**, 689–711, doi:10.1007/s10495-015-1109-1 (2015).
13. Hengartner, M. O. The biochemistry of apoptosis. Nature **407**, 770–776, doi:10.1038/35037710 (2000).
14. Yang, G. J. *et al.* An optimized BRD4 inhibitor effectively eliminates NF-κB-driven triple-negative breast cancer cells. Bioorg Chem **114**, 105158, doi:10.1016/j.bioorg.2021.105158 (2021).
15. Yang, G. J., Ko, C. N., Zhong, H. J., Leung, C. H. & Ma, D. L. Structure-Based Discovery of a Selective KDM5A Inhibitor that Exhibits Anti-Cancer Activity via Inducing Cell Cycle Arrest and Senescence in Breast Cancer Cell Lines. Cancers (Basel) **11**, doi:10.3390/cancers11010092 (2019).
16. Wali, J. A., Masters, S. L. & Thomas, H. E. Linking metabolic abnormalities to apoptotic pathways in Beta cells in type 2 diabetes. Cells **2**, 266–283, doi:10.3390/cells2020266 (2013).
17. Galadari, S., Rahman, A., Pallichankandy, S. & Thayyullathil, F. Molecular targets and anticancer potential of sanguinarine-a benzophenanthridine alkaloid. Phytomedicine **34**, 143–153,

doi:10.1016/j.phymed.2017.08.006 (2017).

18. Jin, S., Zhang, Q. Y., Kang, X. M., Wang, J. X. & Zhao, W. H. Daidzein induces MCF-7 breast cancer cell apoptosis via the mitochondrial pathway. Ann Oncol **21**, 263–268, doi:10.1093/annonc/mdp499 (2010).
19. Caldon, C. E., Daly, R. J., Sutherland, R. L. & Musgrove, E. A. Cell cycle control in breast cancer cells. J Cell Biochem **97**, 261–274, doi:10.1002/jcb.20690 (2006).
20. Lee, T. K. *et al.* Sanguinarine Induces Apoptosis of Human Oral Squamous Cell Carcinoma KB Cells via Inactivation of the PI3K/Akt Signaling Pathway. Drug Dev Res **77**, 227–240, doi:10.1002/ddr.21315 (2016).
21. Achkar, I. W., Mraiche, F., Mohammad, R. M. & Uddin, S. Anticancer potential of sanguinarine for various human malignancies. Future Med Chem **9**, 933–950, doi:10.4155/fmc-2017-0041 (2017).
22. Khan, A. Q. *et al.* Sanguinarine Induces Apoptosis in Papillary Thyroid Cancer Cells via Generation of Reactive Oxygen Species. Molecules **25**, doi:10.3390/molecules25051229 (2020).
23. Kuttikrishnan, S. *et al.* Sanguinarine suppresses growth and induces apoptosis in childhood acute lymphoblastic leukemia. Leuk Lymphoma **60**, 782–794, doi:10.1080/10428194.2018.1494270 (2019).
24. Gong, X. *et al.* Sanguinarine triggers intrinsic apoptosis to suppress colorectal cancer growth through disassociation between STRAP and MELK. BMC Cancer **18**, 578, doi:10.1186/s12885-018-4463-x (2018).
25. Adhami, V. M. *et al.* Sanguinarine causes cell cycle blockade and apoptosis of human prostate carcinoma cells via modulation of cyclin kinase inhibitor-cyclin-cyclin-dependent kinase machinery. Mol Cancer Ther **3**, 933–940 (2004).
26. Debiton, E., Madelmont, J. C., Legault, J. & Barthomeuf, C. Sanguinarine-induced apoptosis is associated with an early and severe cellular glutathione depletion. Cancer Chemother Pharmacol **51**, 474–482, doi:10.1007/s00280-003-0609-9 (2003).
27. Sun, M. *et al.* Sanguinarine suppresses prostate tumor growth and inhibits survivin expression. Genes Cancer **1**, 283–292, doi:10.1177/1947601910368849 (2010).
28. Gu, S. *et al.* Sanguinarine-induced apoptosis in lung adenocarcinoma cells is dependent on reactive oxygen species production and endoplasmic reticulum stress. Oncol Rep **34**, 913–919, doi:10.3892/or.2015.4054 (2015).
29. Jang, B. C. *et al.* Sanguinarine induces apoptosis in A549 human lung cancer cells primarily via cellular glutathione depletion. Toxicol In Vitro **23**, 281–287, doi:10.1016/j.tiv.2008.12.013 (2009).
30. Ding, Z. *et al.* The alkaloid sanguinarine is effective against multidrug resistance in human cervical cells via bimodal cell death. Biochem Pharmacol **63**, 1415–1421, doi:10.1016/s0006-2952(02)00902-4 (2002).
31. Han, M. H. *et al.* Apoptosis induction of human bladder cancer cells by sanguinarine through reactive oxygen species-mediated up-regulation of early growth response gene-1. PLoS One **8**, e63425, doi:10.1371/journal.pone.0063425 (2013).

32. Han, M. H., Kim, G. Y., Yoo, Y. H. & Choi, Y. H. Sanguinarine induces apoptosis in human colorectal cancer HCT-116 cells through ROS-mediated Egr-1 activation and mitochondrial dysfunction. Toxicol Lett **220**, 157–166, doi:10.1016/j.toxlet.2013.04.020 (2013).
33. Lee, J. S., Jung, W. K., Jeong, M. H., Yoon, T. R. & Kim, H. K. Sanguinarine induces apoptosis of HT-29 human colon cancer cells via the regulation of Bax/Bcl-2 ratio and caspase-9-dependent pathway. Int J Toxicol **31**, 70–77, doi:10.1177/1091581811423845 (2012).
34. Xu, J. Y. *et al.* Sanguinarine inhibits growth of human cervical cancer cells through the induction of apoptosis. Oncol Rep **28**, 2264–2270, doi:10.3892/or.2012.2024 (2012).
35. Park, H. *et al.* Sanguinarine induces apoptosis of human osteosarcoma cells through the extrinsic and intrinsic pathways. Biochem Biophys Res Commun **399**, 446–451, doi:10.1016/j.bbrc.2010.07.114 (2010).
36. Han, M. H., Yoo, Y. H. & Choi, Y. H. Sanguinarine-induced apoptosis in human leukemia U937 cells via Bcl-2 downregulation and caspase-3 activation. Chemotherapy **54**, 157–165, doi:10.1159/000140359 (2008).
37. Hussain, A. R. *et al.* Sanguinarine-dependent induction of apoptosis in primary effusion lymphoma cells. Cancer Res **67**, 3888–3897, doi:10.1158/0008-5472.Can-06-3764 (2007).
38. Rahman, A., Thayyullathil, F., Pallichankandy, S. & Galadari, S. Hydrogen peroxide/ceramide/Akt signaling axis play a critical role in the antileukemic potential of sanguinarine. Free Radic Biol Med **96**, 273–289, doi:10.1016/j.freeradbiomed.2016.05.001 (2016).
39. Ahmad, N., Gupta, S., Husain, M. M., Heiskanen, K. M. & Mukhtar, H. Differential antiproliferative and apoptotic response of sanguinarine for cancer cells versus normal cells. Clin Cancer Res **6**, 1524–1528 (2000).
40. Hammerová, J., Uldrijan, S., Táborská, E. & Slaninová, I. Benzo[c]phenanthridine alkaloids exhibit strong anti-proliferative activity in malignant melanoma cells regardless of their p53 status. J Dermatol Sci **62**, 22–35, doi:10.1016/j.jdermsci.2011.01.006 (2011).
41. Rosen, J. *et al.* Characterization and assessment of nanoencapsulated sanguinarine chloride as a potential treatment for melanoma. J Drugs Dermatol **14**, 453–458 (2015).
42. Ahsan, H., Reagan-Shaw, S., Breur, J. & Ahmad, N. Sanguinarine induces apoptosis of human pancreatic carcinoma AsPC-1 and BxPC-3 cells via modulations in Bcl-2 family proteins. Cancer Lett **249**, 198–208, doi:10.1016/j.canlet.2006.08.018 (2007).
43. Fan, H. N. *et al.* Sanguinarine inhibits the tumorigenesis of gastric cancer by regulating the TOX/DNA-PKcs/ KU70/80 pathway. Pathol Res Pract **215**, 152677, doi:10.1016/j.prp.2019.152677 (2019).
44. Cecen, E., Altun, Z., Ercetin, P., Aktas, S. & Olgun, N. Promoting effects of sanguinarine on apoptotic gene expression in human neuroblastoma cells. Asian Pac J Cancer Prev **15**, 9445–9451, doi:10.7314/apjcp.2014.15.21.9445 (2014).
45. Han, M. H. *et al.* Induction of apoptosis by sanguinarine in C6 rat glioblastoma cells is associated with the modulation of the Bcl-2 family and activation of caspases through downregulation of

extracellular signal-regulated kinase and Akt. Anticancer Drugs **18**, 913–921, doi:10.1097/CAD.0b013e328117f463 (2007).

46. Chang, M. C. *et al.* Induction of necrosis and apoptosis to KB cancer cells by sanguinarine is associated with reactive oxygen species production and mitochondrial membrane depolarization. Toxicol Appl Pharmacol **218**, 143–151, doi:10.1016/j.taap.2006.10.025 (2007).
47. Du, Y., Wang, X., Li, C., Jiao, L. & Hu, Y. Effect of Sanguinarine chloride on proliferation and apoptosis of human tongue cancer cells and its mechanism. Panminerva Med, doi:10.23736/s0031-0808.20.04039-2 (2020).
48. Holy, J., Lamont, G. & Perkins, E. Disruption of nucleocytoplasmic trafficking of cyclin D1 and topoisomerase II by sanguinarine. BMC Cell Biol **7**, 13, doi:10.1186/1471-2121-7-13 (2006).
49. Choi, W. Y., Kim, G. Y., Lee, W. H. & Choi, Y. H. Sanguinarine, a benzophenanthridine alkaloid, induces apoptosis in MDA-MB-231 human breast carcinoma cells through a reactive oxygen species-mediated mitochondrial pathway. Chemotherapy **54**, 279–287, doi:10.1159/000149719 (2008).
50. Dong, X. Z. *et al.* Sanguinarine inhibits vascular endothelial growth factor release by generation of reactive oxygen species in MCF-7 human mammary adenocarcinoma cells. *Biomed Res Int* 2013, 517698, doi:10.1155/2013/517698 (2013).
51. Kalogris, C. *et al.* Sanguinarine suppresses basal-like breast cancer growth through dihydrofolate reductase inhibition. Biochem Pharmacol **90**, 226–234, doi:10.1016/j.bcp.2014.05.014 (2014).
52. Kim, S. *et al.* Sanguinarine-induced apoptosis: generation of ROS, down-regulation of Bcl-2, c-FLIP, and synergy with TRAIL. J Cell Biochem **104**, 895–907, doi:10.1002/jcb.21672 (2008).
53. Akhtar, S. *et al.* Sanguinarine Induces Apoptosis Pathway in Multiple Myeloma Cell Lines via Inhibition of the JaK2/STAT3 Signaling. Front Oncol **9**, 285, doi:10.3389/fonc.2019.00285 (2019).
54. Basu, P. & Kumar, G. S. Sanguinarine and Its Role in Chronic Diseases. Adv Exp Med Biol **928**, 155–172, doi:10.1007/978-3-319-41334-1_7 (2016).
55. Chou, T. C. Drug combination studies and their synergy quantification using the Chou-Talalay method. Cancer Res **70**, 440–446, doi:10.1158/0008-5472.Can-09-1947 (2010).
56. Gatti, L. *et al.* Improved apoptotic cell death in drug-resistant non-small-cell lung cancer cells by tumor necrosis factor-related apoptosis-inducing ligand-based treatment. J Pharmacol Exp Ther **348**, 360–371, doi:10.1124/jpet.113.210054 (2014).
57. Choi, W. Y. *et al.* Sanguinarine sensitizes human gastric adenocarcinoma AGS cells to TRAIL-mediated apoptosis via down-regulation of AKT and activation of caspase-3. Anticancer Res **29**, 4457–4465 (2009).
58. Eid, S. Y., El-Readi, M. Z. & Wink, M. Synergism of three-drug combinations of sanguinarine and other plant secondary metabolites with digitonin and doxorubicin in multi-drug resistant cancer cells. Phytomedicine **19**, 1288–1297, doi:10.1016/j.phymed.2012.08.010 (2012).
59. Eid, S. Y., El-Readi, M. Z. & Wink, M. Digitonin synergistically enhances the cytotoxicity of plant secondary metabolites in cancer cells. Phytomedicine **19**, 1307–1314, doi:10.1016/j.phymed.2012.09.002 (2012).

60. Messeha, S. S., Zarmouh, N. O., Asiri, A. & Soliman, K. F. A. Gene Expression Alterations Associated with Oleuropein-Induced Antiproliferative Effects and S-Phase Cell Cycle Arrest in Triple-Negative Breast Cancer Cells. *Nutrients* **12**, doi:10.3390/nu12123755 (2020).
61. Ramachandran, C. *et al.* Expression profiles of apoptotic genes induced by curcumin in human breast cancer and mammary epithelial cell lines. Anticancer Res **25**, 3293–3302 (2005).
62. Rahman, K. W., Li, Y., Wang, Z., Sarkar, S. H. & Sarkar, F. H. Gene expression profiling revealed survivin as a target of 3,3'-diindolylmethane-induced cell growth inhibition and apoptosis in breast cancer cells. Cancer Res **66**, 4952–4960, doi:10.1158/0008-5472.Can-05-3918 (2006).
63. Adhami, V. M., Aziz, M. H., Mukhtar, H. & Ahmad, N. Activation of prodeath Bcl-2 family proteins and mitochondrial apoptosis pathway by sanguinarine in immortalized human HaCaT keratinocytes. Clin Cancer Res **9**, 3176–3182 (2003).
64. Weerasinghe, P., Hallock, S. & Liepins, A. Bax, Bcl-2, and NF-kappaB expression in sanguinarine induced bimodal cell death. Exp Mol Pathol **71**, 89–98, doi:10.1006/exmp.2001.2355 (2001).
65. Weerasinghe, P., Hallock, S., Tang, S. C. & Liepins, A. Role of Bcl-2 family proteins and caspase-3 in sanguinarine-induced bimodal cell death. Cell Biol Toxicol **17**, 371–381, doi:10.1023/a:1013796432521 (2001).
66. Weerasinghe, P., Hallock, S., Tang, S. C. & Liepins, A. Sanguinarine induces bimodal cell death in K562 but not in high Bcl-2-expressing JM1 cells. Pathol Res Pract **197**, 717–726, doi:10.1078/0344-0338-00150 (2001).
67. Weerasinghe, P., Hallock, S., Tang, S. C., Trump, B. & Liepins, A. Sanguinarine overcomes P-glycoprotein-mediated multidrug-resistance via induction of apoptosis and oncosis in CEM-VLB 1000 cells. Exp Toxicol Pathol **58**, 21–30, doi:10.1016/j.etp.2006.01.008 (2006).
68. Xu, J. *et al.* AKT Degradation Selectively Inhibits the Growth of PI3K/PTEN Pathway-Mutant Cancers with Wild-Type KRAS and BRAF by Destabilizing Aurora Kinase B. Cancer Discov, doi:10.1158/2159-8290.Cd-20-0815 (2021).
69. Morris, G. J. *et al.* Differences in breast carcinoma characteristics in newly diagnosed African-American and Caucasian patients: a single-institution compilation compared with the National Cancer Institute's Surveillance, Epidemiology, and End Results database. Cancer **110**, 876–884, doi:10.1002/cncr.22836 (2007).
70. Jemal, A. *et al.* Annual report to the nation on the status of cancer, 1975–2001, with a special feature regarding survival. *Cancer* **101**, 3–27, doi:10.1002/cncr.20288 (2004).
71. Tate, C. R. *et al.* Targeting triple-negative breast cancer cells with the histone deacetylase inhibitor panobinostat. Breast Cancer Res **14**, R79, doi:10.1186/bcr3192 (2012).
72. El Guerrab, A. *et al.* Anti-EGFR monoclonal antibodies and EGFR tyrosine kinase inhibitors as combination therapy for triple-negative breast cancer. Oncotarget **7**, 73618–73637, doi:10.18632/oncotarget.12037 (2016).
73. Pylayeva, Y. *et al.* Ras- and PI3K-dependent breast tumorigenesis in mice and humans requires focal adhesion kinase signaling. J Clin Invest **119**, 252–266, doi:10.1172/jci37160 (2009).

74. Huo, D. *et al.* Comparison of Breast Cancer Molecular Features and Survival by African and European Ancestry in The Cancer Genome Atlas. JAMA Oncol **3**, 1654–1662, doi:10.1001/jamaoncol.2017.0595 (2017).
75. Dietze, E. C., Sistrunk, C., Miranda-Carboni, G., O'Regan, R. & Seewaldt, V. L. Triple-negative breast cancer in African-American women: disparities versus biology. Nat Rev Cancer **15**, 248–254, doi:10.1038/nrc3896 (2015).
76. Yoshida, K. & Miki, Y. Role of BRCA1 and BRCA2 as regulators of DNA repair, transcription, and cell cycle in response to DNA damage. Cancer Sci **95**, 866–871, doi:10.1111/j.1349-7006.2004.tb02195.x (2004).
77. Vermeulen, K., Berneman, Z. N. & Van Bockstaele, D. R. Cell cycle and apoptosis. Cell Prolif **36**, 165–175, doi:10.1046/j.1365-2184.2003.00267.x (2003).
78. Malumbres, M. Cyclin-dependent kinases. Genome Biol **15**, 122, doi:10.1186/gb4184 (2014).
79. Wu, H. *et al.* The Cytotoxicity Effect of Resveratrol: Cell Cycle Arrest and Induced Apoptosis of Breast Cancer 4T1 Cells. Toxins (Basel) **11**, doi:10.3390/toxins11120731 (2019).
80. Man, S. M. & Kanneganti, T. D. Converging roles of caspases in inflammasome activation, cell death and innate immunity. Nat Rev Immunol **16**, 7–21, doi:10.1038/nri.2015.7 (2016).
81. McIlwain, D. R., Berger, T. & Mak, T. W. Caspase functions in cell death and disease. Cold Spring Harb Perspect Biol **7**, doi:10.1101/cshperspect.a026716 (2015).
82. Yazdi, A. S., Guarda, G., D'Ombrain, M. C. & Drexler, S. K. Inflammatory caspases in innate immunity and inflammation. J Innate Immun **2**, 228–237, doi:10.1159/000283688 (2010).
83. Sun, Y. & Guo, Y. Expression of Caspase-1 in breast cancer tissues and its effects on cell proliferation, apoptosis and invasion. Oncol Lett **15**, 6431–6435, doi:10.3892/ol.2018.8176 (2018).
84. Miura, M., Zhu, H., Rotello, R., Hartwieg, E. A. & Yuan, J. Induction of apoptosis in fibroblasts by IL-1 beta-converting enzyme, a mammalian homolog of the C. elegans cell death gene ced-3. Cell **75**, 653–660, doi:10.1016/0092-8674(93)90486-a (1993).
85. Engels, I. H., Totzke, G., Fischer, U., Schulze-Osthoff, K. & Jänicke, R. U. Caspase-10 sensitizes breast carcinoma cells to TRAIL-induced but not tumor necrosis factor-induced apoptosis in a caspase-3-dependent manner. Mol Cell Biol **25**, 2808–2818, doi:10.1128/mcb.25.7.2808-2818.2005 (2005).
86. Tait, S. W. & Green, D. R. Mitochondria and cell death: outer membrane permeabilization and beyond. Nat Rev Mol Cell Biol **11**, 621–632, doi:10.1038/nrm2952 (2010).
87. Kang, S. J. *et al.* Dual role of caspase-11 in mediating activation of caspase-1 and caspase-3 under pathological conditions. J Cell Biol **149**, 613–622, doi:10.1083/jcb.149.3.613 (2000).
88. Guégan, C. *et al.* Instrumental activation of bid by caspase-1 in a transgenic mouse model of ALS. Mol Cell Neurosci **20**, 553–562, doi:10.1006/mcne.2002.1136 (2002).
89. Faridi, U. *et al.* Repurposing L-Menthol for Systems Medicine and Cancer Therapeutics? L-Menthol Induces Apoptosis through Caspase 10 and by Suppressing HSP90. Omics **20**, 53–64, doi:10.1089/omi.2015.0118 (2016).

90. Kesavardhana, S., Malireddi, R. K. S. & Kanneganti, T. D. Caspases in Cell Death, Inflammation, and Pyroptosis. Annu Rev Immunol **38**, 567–595, doi:10.1146/annurev-immunol-073119-095439 (2020).
91. Youle, R. J. & Strasser, A. The BCL-2 protein family: opposing activities that mediate cell death. Nat Rev Mol Cell Biol **9**, 47–59, doi:10.1038/nrm2308 (2008).
92. Miyashita, T. *et al.* Tumor suppressor p53 is a regulator of bcl-2 and bax gene expression in vitro and in vivo. Oncogene **9**, 1799–1805 (1994).
93. Akiyama, T., Dass, C. R. & Choong, P. F. Bim-targeted cancer therapy: a link between drug action and underlying molecular changes. Mol Cancer Ther **8**, 3173–3180, doi:10.1158/1535-7163.Mct-09-0685 (2009).
94. Shukla, S., Saxena, S., Singh, B. K. & Kakkar, P. BH3-only protein BIM: An emerging target in chemotherapy. Eur J Cell Biol **96**, 728–738, doi:10.1016/j.ejcb.2017.09.002 (2017).
95. Butt, A. J. *et al.* A novel plant toxin, persin, with in vivo activity in the mammary gland, induces Bim-dependent apoptosis in human breast cancer cells. Mol Cancer Ther **5**, 2300–2309, doi:10.1158/1535-7163.Mct-06-0170 (2006).
96. Hafezi, S. & Rahmani, M. Targeting BCL-2 in Cancer: Advances, Challenges, and Perspectives. Cancers (Basel) **13**, doi:10.3390/cancers13061292 (2021).
97. Dai, Y. & Grant, S. BCL2L11/Bim as a dual-agent regulating autophagy and apoptosis in drug resistance. Autophagy **11**, 416–418, doi:10.1080/15548627.2014.998892 (2015).
98. Sur, S., Steele, R., Shi, X. & Ray, R. B. miRNA-29b Inhibits Prostate Tumor Growth and Induces Apoptosis by Increasing Bim Expression. Cells **8**, doi:10.3390/cells8111455 (2019).
99. Yang, M. C. *et al.* Bim directly antagonizes Bcl-xl in doxorubicin-induced prostate cancer cell apoptosis independently of p53. Cell Cycle **15**, 394–402, doi:10.1080/15384101.2015.1127470 (2016).
100. Imazu, T. *et al.* Bcl-2/E1B 19 kDa-interacting protein 3-like protein (Bnip3L) interacts with bcl-2/Bcl-xL and induces apoptosis by altering mitochondrial membrane permeability. Oncogene **18**, 4523–4529, doi:10.1038/sj.onc.1202722 (1999).
101. Inohara, N., Ding, L., Chen, S. & Núñez, G. harakiri, a novel regulator of cell death, encodes a protein that activates apoptosis and interacts selectively with survival-promoting proteins Bcl-2 and Bcl-X(L). Embo j **16**, 1686–1694, doi:10.1093/emboj/16.7.1686 (1997).
102. Kaya-Aksoy, E. *et al.* The pro-apoptotic Bcl-2 family member Harakiri (HRK) induces cell death in glioblastoma multiforme. Cell Death Discov **5**, 64, doi:10.1038/s41420-019-0144-z (2019).
103. Lin, J. *et al.* Suppression activity of pro-apoptotic gene products in cancer cells, a potential application for cancer gene therapy. Anticancer Res **21**, 831–839 (2001).
104. Yip, N. K. & Ho, W. S. Berberine induces apoptosis via the mitochondrial pathway in liver cancer cells. Oncol Rep **30**, 1107–1112, doi:10.3892/or.2013.2543 (2013).
105. Chang, I. *et al.* Hrk mediates 2-methoxyestradiol-induced mitochondrial apoptotic signaling in prostate cancer cells. Mol Cancer Ther **12**, 1049–1059, doi:10.1158/1535-7163.Mct-12-1187 (2013).

106. Messeha, S. S., Zarmouh, N. O., Asiri, A. & Soliman, K. F. A. Rosmarinic acid-induced apoptosis and cell cycle arrest in triple-negative breast cancer cells. Eur J Pharmacol **885**, 173419, doi:10.1016/j.ejphar.2020.173419 (2020).
107. Malíková, J., Zdarilová, A., Hlobilková, A. & Ulrichová, J. The effect of chelerythrine on cell growth, apoptosis, and cell cycle in human normal and cancer cells in comparison with sanguinarine. Cell Biol Toxicol **22**, 439–453, doi:10.1007/s10565-006-0109-x (2006).
108. Philchenkov, A., Kaminskyy, V., Zavelevich, M. & Stoika, R. Apoptogenic activity of two benzophenanthridine alkaloids from Chelidonium majus L. does not correlate with their DNA damaging effects. Toxicol In Vitro **22**, 287–295, doi:10.1016/j.tiv.2007.08.023 (2008).
109. Schattner, E. J. Apoptosis in lymphocytic leukemias and lymphomas. Cancer Invest **20**, 737–748, doi:10.1081/cnv-120002951 (2002).
110. Vogler, M. BCL2A1: the underdog in the BCL2 family. Cell Death Differ **19**, 67–74, doi:10.1038/cdd.2011.158 (2012).
111. Hiraki, M. *et al.* Targeting MUC1-C suppresses BCL2A1 in triple-negative breast cancer. Signal Transduct Target Ther **3**, 13, doi:10.1038/s41392-018-0013-x (2018).
112. Karczmarek-Borowska, B. *et al.* Estimation of prognostic value of Bcl-xL gene expression in non-small cell lung cancer. Lung Cancer **51**, 61–69, doi:10.1016/j.lungcan.2005.08.010 (2006).
113. Olopade, O. I. *et al.* Overexpression of BCL-x protein in primary breast cancer is associated with high tumor grade and nodal metastases. Cancer J Sci Am **3**, 230–237 (1997).
114. Watanabe, J. *et al.* Bcl-xL overexpression in human hepatocellular carcinoma. Int J Oncol **21**, 515–519 (2002).
115. Keitel, U. *et al.* Bcl-xL mediates therapeutic resistance of a mesenchymal breast cancer cell subpopulation. Oncotarget **5**, 11778–11791, doi:10.18632/oncotarget.2634 (2014).
116. Martin, S. S. *et al.* A cytoskeleton-based functional genetic screen identifies Bcl-xL as an enhancer of metastasis, but not primary tumor growth. Oncogene **23**, 4641–4645, doi:10.1038/sj.onc.1207595 (2004).
117. Bessou, M. *et al.* The apoptosis inhibitor Bcl-xL controls breast cancer cell migration through mitochondria-dependent reactive oxygen species production. Oncogene **39**, 3056–3074, doi:10.1038/s41388-020-1212-9 (2020).
118. Fernández, Y., España, L., Mañas, S., Fabra, A. & Sierra, A. Bcl-xL promotes metastasis of breast cancer cells by induction of cytokines resistance. Cell Death Differ **7**, 350–359, doi:10.1038/sj.cdd.4400662 (2000).
119. Pirouzpanah, M. B., Sabzichi, M., Pirouzpanah, S., Chavoshi, H. & Samadi, N. Silibilin-induces apoptosis in breast cancer cells by modulating p53, p21, Bak and Bcl-XL pathways. Asian Pac J Cancer Prev **16**, 2087–2092, doi:10.7314/apjcp.2015.16.5.2087 (2015).
120. Sharifi, S., Barar, J., Hejazi, M. S. & Samadi, N. Doxorubicin Changes Bax /Bcl-xL Ratio, Caspase-8 and 9 in Breast Cancer Cells. Adv Pharm Bull **5**, 351–359, doi:10.15171/apb.2015.049 (2015).

121. Simões-Wüst, A. P. *et al.* Bcl-xl antisense treatment induces apoptosis in breast carcinoma cells. Int J Cancer **87**, 582–590, doi:10.1002/1097-0215(20000815)87:4<582::aid-ijc19>3.0.co;2-p (2000).
122. Lin, H., Koren, S. A., Cvetojevic, G., Girardi, P. & Johnson, G. V. W. The role of BAG3 in health and disease: A "Magic BAG of Tricks". J Cell Biochem, doi:10.1002/jcb.29952 (2021).
123. Festa, M. *et al.* BAG3 protein is overexpressed in human glioblastoma and is a potential target for therapy. Am J Pathol **178**, 2504–2512, doi:10.1016/j.ajpath.2011.02.002 (2011).
124. Chiappetta, G. *et al.* The antiapoptotic protein BAG3 is expressed in thyroid carcinomas and modulates apoptosis mediated by tumor necrosis factor-related apoptosis-inducing ligand. J Clin Endocrinol Metab **92**, 1159–1163, doi:10.1210/jc.2006-1712 (2007).
125. Chiappetta, G. *et al.* The anti-apoptotic BAG3 protein is expressed in lung carcinomas and regulates small cell lung carcinoma (SCLC) tumor growth. Oncotarget **5**, 6846–6853, doi:10.18632/oncotarget.2261 (2014).
126. Das, C. K. *et al.* BAG3 Overexpression and Cytoprotective Autophagy Mediate Apoptosis Resistance in Chemoresistant Breast Cancer Cells. Neoplasia **20**, 263–279, doi:10.1016/j.neo.2018.01.001 (2018).
127. Liu, B. Q. *et al.* BAG3 promotes stem cell-like phenotype in breast cancer by upregulation of CXCR4 via interaction with its transcript. Cell Death Dis **8**, e2933, doi:10.1038/cddis.2017.324 (2017).
128. Karpel-Massler, G. *et al.* Combined inhibition of Bcl-2/Bcl-xL and Usp9X/Bag3 overcomes apoptotic resistance in glioblastoma in vitro and in vivo. Oncotarget **6**, 14507–14521, doi:10.18632/oncotarget.3993 (2015).
129. Furusawa, Y. *et al.* Identification of genes and genetic networks associated with BAG3dependent cell proliferation and cell survival in human cervical cancer HeLa cells. Mol Med Rep **18**, 4138–4146, doi:10.3892/mmr.2018.9383 (2018).
130. Li, C. *et al.* BAG3 regulates stability of IL-8 mRNA via interplay between HuR and miR-4312 in PDACs. Cell Death Dis **9**, 863, doi:10.1038/s41419-018-0874-5 (2018).
131. Peták, I. & Houghton, J. A. Shared pathways: death receptors and cytotoxic drugs in cancer therapy. Pathol Oncol Res **7**, 95–106, doi:10.1007/bf03032574 (2001).
132. Cao, X., Pobezinskaya, Y. L., Morgan, M. J. & Liu, Z. G. The role of TRADD in TRAIL-induced apoptosis and signaling. Faseb j **25**, 1353–1358, doi:10.1096/fj.10-170480 (2011).
133. Walczak, H. Death receptor-ligand systems in cancer, cell death, and inflammation. Cold Spring Harb Perspect Biol **5**, a008698, doi:10.1101/cshperspect.a008698 (2013).
134. Dumont, P. *et al.* The Amaryllidaceae isocarbostyril narciclasine induces apoptosis by activation of the death receptor and/or mitochondrial pathways in cancer cells but not in normal fibroblasts. Neoplasia **9**, 766–776, doi:10.1593/neo.07535 (2007).
135. Chinnaiyan, A. M. *et al.* Signal transduction by DR3, a death domain-containing receptor related to TNFR-1 and CD95. Science **274**, 990–992, doi:10.1126/science.274.5289.990 (1996).

136. Kitson, J. *et al.* A death-domain-containing receptor that mediates apoptosis. Nature **384**, 372–375, doi:10.1038/384372a0 (1996).

137. Xu, Z. *et al.* Roles of TNF receptor-associated and Fas-associated death domain proteins in the apoptosis of Eimeria tenella host cells. Vet Parasitol **290**, 109351, doi:10.1016/j.vetpar.2021.109351 (2021).

138. Füllsack, S., Rosenthal, A., Wajant, H. & Siegmund, D. Redundant and receptor-specific activities of TRADD, RIPK1 and FADD in death receptor signaling. Cell Death Dis **10**, 122, doi:10.1038/s41419-019-1396-5 (2019).

139. Sprick, M. R. *et al.* FADD/MORT1 and caspase-8 are recruited to TRAIL receptors 1 and 2 and are essential for apoptosis mediated by TRAIL receptor 2. *Immunity* **12**, 599–609, doi:10.1016/s1074-7613(00)80211-3 (2000).

140. Silva, J. C. *et al.* Apoptosis-associated genes related to photodynamic therapy in breast carcinomas. Lasers Med Sci **29**, 1429–1436, doi:10.1007/s10103-014-1547-y (2014).

141. Johnstone, R. W., Frew, A. J. & Smyth, M. J. The TRAIL apoptotic pathway in cancer onset, progression and therapy. Nat Rev Cancer **8**, 782–798, doi:10.1038/nrc2465 (2008).

142. Matsuyoshi, S., Shimada, K., Nakamura, M., Ishida, E. & Konishi, N. FADD phosphorylation is critical for cell cycle regulation in breast cancer cells. Br J Cancer **94**, 532–539, doi:10.1038/sj.bjc.6602955 (2006).

143. Dong, Y., Wu, Y., Cui, M. Z. & Xu, X. Lysophosphatidic Acid Triggers Apoptosis in HeLa Cells through the Upregulation of Tumor Necrosis Factor Receptor Superfamily Member 21. *Mediators Inflamm* 2017, 2754756, doi:10.1155/2017/2754756 (2017).

144. Zeng, L. *et al.* Death receptor 6 induces apoptosis not through type I or type II pathways, but via a unique mitochondria-dependent pathway by interacting with Bax protein. J Biol Chem **287**, 29125–29133, doi:10.1074/jbc.M112.362038 (2012).

145. Karl, I. *et al.* TRAF2 inhibits TRAIL- and CD95L-induced apoptosis and necroptosis. Cell Death Dis **5**, e1444, doi:10.1038/cddis.2014.404 (2014).

146. Tsuchida, M. *et al.* Pro-apoptotic functions of TRAF2 in p53-mediated apoptosis induced by cisplatin. J Toxicol Sci **45**, 219–226, doi:10.2131/jts.45.219 (2020).

147. Holen, I. *et al.* Osteoprotegerin (OPG) expression by breast cancer cells in vitro and breast tumours in vivo–a role in tumour cell survival? Breast Cancer Res Treat **92**, 207–215, doi:10.1007/s10549-005-2419-8 (2005).

148. Holen, I. & Shipman, C. M. Role of osteoprotegerin (OPG) in cancer. Clin Sci (Lond) **110**, 279–291, doi:10.1042/cs20050175 (2006).

149. Weichhaus, M., Segaran, P., Renaud, A., Geerts, D. & Connelly, L. Osteoprotegerin expression in triple-negative breast cancer cells promotes metastasis. Cancer Med **3**, 1112–1125, doi:10.1002/cam4.277 (2014).

150. Ito, R. *et al.* Expression of osteoprotegerin correlates with aggressiveness and poor prognosis of gastric carcinoma. Virchows Arch **443**, 146–151, doi:10.1007/s00428-003-0845-8 (2003).

151. König, C., Hillert-Richter, L. K., Ivanisenko, N. V., Ivanisenko, V. A. & Lavrik, I. N. Pharmacological targeting of c-FLIP(L) and Bcl-2 family members promotes apoptosis in CD95L-resistant cells. Sci Rep **10**, 20823, doi:10.1038/s41598-020-76079-1 (2020).
152. Hughes, M. A. *et al.* Co-operative and Hierarchical Binding of c-FLIP and Caspase-8: A Unified Model Defines How c-FLIP Isoforms Differentially Control Cell Fate. Mol Cell **61**, 834–849, doi:10.1016/j.molcel.2016.02.023 (2016).
153. Wajant, H. Targeting the FLICE Inhibitory Protein (FLIP) in cancer therapy. Mol Interv **3**, 124–127, doi:10.1124/mi.3.3.124 (2003).
154. Fianco, G. *et al.* Caspase-8: A Novel Target to Overcome Resistance to Chemotherapy in Glioblastoma. Int J Mol Sci **19**, doi:10.3390/ijms19123798 (2018).
155. Liang, J. *et al.* Comprehensive molecular characterization of inhibitors of apoptosis proteins (IAPs) for therapeutic targeting in cancer. BMC Med Genomics **13**, 7, doi:10.1186/s12920-020-0661-x (2020).
156. Frazzi, R. BIRC3 and BIRC5: multi-faceted inhibitors in cancer. Cell Biosci **11**, 8, doi:10.1186/s13578-020-00521-0 (2021).
157. Hunter, A. M., LaCasse, E. C. & Korneluk, R. G. The inhibitors of apoptosis (IAPs) as cancer targets. Apoptosis **12**, 1543–1568, doi:10.1007/s10495-007-0087-3 (2007).
158. Jha, K., Shukla, M. & Pandey, M. Survivin expression and targeting in breast cancer. Surg Oncol **21**, 125–131, doi:10.1016/j.suronc.2011.01.001 (2012).
159. Wang, L. *et al.* LncRNA HCP5 promotes triple negative breast cancer progression as a ceRNA to regulate BIRC3 by sponging miR-219a-5p. Cancer Med **8**, 4389–4403, doi:10.1002/cam4.2335 (2019).
160. Srour, M. K. *et al.* Gene expression comparison between primary triple-negative breast cancer and paired axillary and sentinel lymph node metastasis. Breast J **26**, 904–910, doi:10.1111/tbj.13684 (2020).
161. Hahm, E. R. & Singh, S. V. Withaferin A-induced apoptosis in human breast cancer cells is associated with suppression of inhibitor of apoptosis family protein expression. Cancer Lett **334**, 101–108, doi:10.1016/j.canlet.2012.08.026 (2013).
162. Lu, W. *et al.* MCPIP1 Selectively Destabilizes Transcripts Associated with an Antiapoptotic Gene Expression Program in Breast Cancer Cells That Can Elicit Complete Tumor Regression. Cancer Res **76**, 1429–1440, doi:10.1158/0008-5472.Can-15-1115 (2016).
163. Mendoza-Rodríguez, M., Arévalo Romero, H., Fuentes-Pananá, E. M., Ayala-Sumuano, J. T. & Meza, I. IL-1β induces up-regulation of BIRC3, a gene involved in chemoresistance to doxorubicin in breast cancer cells. Cancer Lett **390**, 39–44, doi:10.1016/j.canlet.2017.01.005 (2017).
164. Stevens, C. *et al.* Peptide combinatorial libraries identify TSC2 as a death-associated protein kinase (DAPK) death domain-binding protein and reveal a stimulatory role for DAPK in mTORC1 signaling. J Biol Chem **284**, 334–344, doi:10.1074/jbc.M805165200 (2009).

165. Bradley, J. R. TNF-mediated inflammatory disease. J Pathol **214**, 149–160, doi:10.1002/path.2287 (2008).

166. Inbal, B., Bialik, S., Sabanay, I., Shani, G. & Kimchi, A. DAP kinase and DRP-1 mediate membrane blebbing and the formation of autophagic vesicles during programmed cell death. J Cell Biol **157**, 455–468, doi:10.1083/jcb.200109094 (2002).

167. Cohen, O., Feinstein, E. & Kimchi, A. DAP-kinase is a Ca2+/calmodulin-dependent, cytoskeletal-associated protein kinase, with cell death-inducing functions that depend on its catalytic activity. Embo j **16**, 998–1008, doi:10.1093/emboj/16.5.998 (1997).

168. Yoo, H. J. *et al.* DAPk1 inhibits NF-κB activation through TNF-α and INF-γ-induced apoptosis. Cell Signal **24**, 1471–1477, doi:10.1016/j.cellsig.2012.03.010 (2012).

169. Raveh, T., Droguett, G., Horwitz, M. S., DePinho, R. A. & Kimchi, A. DAP kinase activates a p19ARF/p53-mediated apoptotic checkpoint to suppress oncogenic transformation. Nat Cell Biol **3**, 1–7, doi:10.1038/35050500 (2001).

170. Arko-Boham, B. *et al.* Prospecting for Breast Cancer Blood Biomarkers: Death-Associated Protein Kinase 1 (DAPK1) as a Potential Candidate. *Dis Markers* 2020, 6848703, doi:10.1155/2020/6848703 (2020).

171. Zhao, J. *et al.* Death-associated protein kinase 1 promotes growth of p53-mutant cancers. J Clin Invest **125**, 2707–2720, doi:10.1172/jci70805 (2015).

172. Liu, X., Zou, H., Slaughter, C. & Wang, X. DFF, a heterodimeric protein that functions downstream of caspase-3 to trigger DNA fragmentation during apoptosis. Cell **89**, 175–184, doi:10.1016/s0092-8674(00)80197-x (1997).

173. Li, H. *et al.* Cell death-inducing DFF45-like effector b (Cideb) is present in pancreatic beta-cells and involved in palmitate induced beta-cell apoptosis. Diabetes Metab Res Rev **28**, 145–155, doi:10.1002/dmrr.1295 (2012).

174. Heim, V. J., Stafford, C. A. & Nachbur, U. NOD Signaling and Cell Death. Front Cell Dev Biol **7**, 208, doi:10.3389/fcell.2019.00208 (2019).

175. Banas, T., Skotniczny, K. & Basta, A. DFF45 expression in ovarian endometriomas. Eur J Obstet Gynecol Reprod Biol **146**, 87–91, doi:10.1016/j.ejogrb.2009.05.024 (2009).

176. Bertin, J. *et al.* Human CARD4 protein is a novel CED-4/Apaf-1 cell death family member that activates NF-kappaB. J Biol Chem **274**, 12955–12958, doi:10.1074/jbc.274.19.12955 (1999).

177. Man, G. C. W. *et al.* Therapeutic potential of a novel prodrug of green tea extract in induction of apoptosis via ERK/JNK and Akt signaling pathway in human endometrial cancer. BMC Cancer **20**, 964, doi:10.1186/s12885-020-07455-3 (2020).

178. da Silva Correia, J. *et al.* Nod1-dependent control of tumor growth. Proc Natl Acad Sci U S A **103**, 1840–1845, doi:10.1073/pnas.0509228103 (2006).

179. McCarthy, J. V., Ni, J. & Dixit, V. M. RIP2 is a novel NF-kappaB-activating and cell death-inducing kinase. J Biol Chem **273**, 16968–16975, doi:10.1074/jbc.273.27.16968 (1998).

180. Wolf, M. J., Seleznik, G. M., Zeller, N. & Heikenwalder, M. The unexpected role of lymphotoxin beta receptor signaling in carcinogenesis: from lymphoid tissue formation to liver and prostate cancer development. Oncogene **29**, 5006–5018, doi:10.1038/onc.2010.260 (2010).
181. Gubernatorova, E. O. *et al.* Dual Role of TNF and LTα in Carcinogenesis as Implicated by Studies in Mice. Cancers (Basel) **13**, doi:10.3390/cancers13081775 (2021).
182. Ito, D., Back, T. C., Shakhov, A. N., Wiltrout, R. H. & Nedospasov, S. A. Mice with a targeted mutation in lymphotoxin-alpha exhibit enhanced tumor growth and metastasis: impaired NK cell development and recruitment. J Immunol **163**, 2809–2815 (1999).
183. Hehlgans, T. *et al.* Lymphotoxin-beta receptor immune interaction promotes tumor growth by inducing angiogenesis. Cancer Res **62**, 4034–4040 (2002).
184. Haybaeck, J. *et al.* A lymphotoxin-driven pathway to hepatocellular carcinoma. Cancer Cell **16**, 295–308, doi:10.1016/j.ccr.2009.08.021 (2009).
185. Lukashev, M. *et al.* Targeting the lymphotoxin-beta receptor with agonist antibodies as a potential cancer therapy. Cancer Res **66**, 9617–9624, doi:10.1158/0008-5472.Can-06-0217 (2006).
186. Fernandes, M. T., Dejardin, E. & dos Santos, N. R. Context-dependent roles for lymphotoxin-β receptor signaling in cancer development. Biochim Biophys Acta **1865**, 204–219, doi:10.1016/j.bbcan.2016.02.005 (2016).
187. Bauer, J. *et al.* Lymphotoxin, NF-κB, and cancer: the dark side of cytokines. Dig Dis **30**, 453–468, doi:10.1159/000341690 (2012).
188. Tront, J. S., Willis, A., Huang, Y., Hoffman, B. & Liebermann, D. A. Gadd45a levels in human breast cancer are hormone receptor dependent. J Transl Med **11**, 131, doi:10.1186/1479-5876-11-131 (2013).
189. Sun, Y., Tang, S. & Xiao, X. The Effect of GADD45a on Furazolidone-Induced S-Phase Cell-Cycle Arrest in Human Hepatoma G2 Cells. J Biochem Mol Toxicol **29**, 489–495, doi:10.1002/jbt.21719 (2015).
190. Yang, Z., Song, L. & Huang, C. Gadd45 proteins as critical signal transducers linking NF-kappaB to MAPK cascades. Curr Cancer Drug Targets **9**, 915–930, doi:10.2174/156800909790192383 (2009).
191. Takekawa, M. & Saito, H. A family of stress-inducible GADD45-like proteins mediate activation of the stress-responsive MTK1/MEKK4 MAPKKK. Cell **95**, 521–530, doi:10.1016/s0092-8674(00)81619-0 (1998).
192. Li, F. H., Han, N., Wang, Y. & Xu, Q. Gadd45a knockdown alleviates oxidative stress through suppressing the p38 MAPK signaling pathway in the pathogenesis of preeclampsia. Placenta **65**, 20–28, doi:10.1016/j.placenta.2018.03.007 (2018).
193. Liu, C., Liu, H., Sun, Q. & Zhang, P. MicroRNA 1283 alleviates cardiomyocyte damage caused by hypoxia /reoxygenation via targeting GADD45A and inactivating the JNK and p38 MAPK signaling pathways. Kardiol Pol **79**, 147–155, doi:10.33963/kp.15696 (2021).
194. Sun, R. X. *et al.* Gadd45α affects retinal ganglion cell injury in chronic ocular hypertension rats by regulating p38MAPK pathway. Gene **763**, 145030, doi:10.1016/j.gene.2020.145030 (2020).

195. Harris, S. L. & Levine, A. J. The p53 pathway: positive and negative feedback loops. Oncogene **24**, 2899–2908, doi:10.1038/sj.onc.1208615 (2005).

196. Lane, D. P. Cancer. p53, guardian of the genome. Nature **358**, 15–16, doi:10.1038/358015a0 (1992).

197. Silwal-Pandit, L., Langerød, A. & Børresen-Dale, A. L. TP53 Mutations in Breast and Ovarian Cancer. Cold Spring Harb Perspect Med **7**, doi:10.1101/cshperspect.a026252 (2017).

198. Qamar, S. *et al.* Association of p53 Overexpression with Hormone Receptor Status and Triple Negative Breast Carcinoma. J Coll Physicians Surg Pak **29**, 164–167, doi:10.29271/jcpsp.2019.02.164 (2019).

199. Finetti, P. *et al.* ESPL1 is a candidate oncogene of luminal B breast cancers. Breast Cancer Res Treat **147**, 51–59, doi:10.1007/s10549-014-3070-z (2014).

200. Kowalczyk, M. C. *et al.* Modulation of biomarkers related to tumor initiation and promotion in mouse skin by a natural β-glucuronidase inhibitor and its precursors. Oncol Rep **26**, 551–556, doi:10.3892/or.2011.1351 (2011).

201. Walaszek, Z. Potential use of D-glucaric acid derivatives in cancer prevention. Cancer Lett **54**, 1–8, doi:10.1016/0304-3835(90)90083-a (1990).

202. Morita, N. *et al.* Effects of synthetic and natural in vivo inhibitors of β-glucuronidase on azoxymethane-induced colon carcinogenesis in rats. Mol Med Rep **1**, 741–746, doi:10.3892/mmr_00000022 (2008).

203. Bhatt, A. P. *et al.* Targeted inhibition of gut bacterial β-glucuronidase activity enhances anticancer drug efficacy. Proc Natl Acad Sci U S A **117**, 7374–7381, doi:10.1073/pnas.1918095117 (2020).

204. Wang, Q., Chen, X. & Hay, N. Akt as a target for cancer therapy: more is not always better (lessons from studies in mice). Br J Cancer **117**, 159–163, doi:10.1038/bjc.2017.153 (2017).

205. Cohen, M. M., Jr. The AKT genes and their roles in various disorders. *Am J Med Genet A* **161a**, 2931–2937, doi:10.1002/ajmg.a.36101 (2013).

206. Martini, M., De Santis, M. C., Braccini, L., Gulluni, F. & Hirsch, E. PI3K/AKT signaling pathway and cancer: an updated review. Ann Med **46**, 372–383, doi:10.3109/07853890.2014.912836 (2014).

207. Wadhwa, B. *et al.* AKT isoforms have discrete expression in triple negative breast cancers and roles in cisplatin sensitivity. Oncotarget **11**, 4178–4194, doi:10.18632/oncotarget.27746 (2020).

208. Dillon, R. L. *et al.* Akt1 and akt2 play distinct roles in the initiation and metastatic phases of mammary tumor progression. Cancer Res **69**, 5057–5064, doi:10.1158/0008-5472.Can-08-4287 (2009).

209. Ju, X. *et al.* Akt1 governs breast cancer progression in vivo. Proc Natl Acad Sci U S A **104**, 7438–7443, doi:10.1073/pnas.0605874104 (2007).

210. Polo, M. L. *et al.* Activation of PI3K/Akt/mTOR signaling in the tumor stroma drives endocrine therapy-dependent breast tumor regression. Oncotarget **6**, 22081–22097, doi:10.18632/oncotarget.4203 (2015).

211. Johnson, J. *et al.* Role of AMPK and Akt in triple negative breast cancer lung colonization. Neoplasia **23**, 429–438, doi:10.1016/j.neo.2021.03.005 (2021).

212. Frankos, V. H. *et al.* Safety of Sanguinaria extract as used in commercial toothpaste and oral rinse products. J Can Dent Assoc **56**, 41–47 (1990).

213. Wang, X. Q., Wang, X. M., Zhou, T. F. & Dong, L. Q. Screening of differentially expressed genes and small molecule drugs of pediatric allergic asthma with DNA microarray. Eur Rev Med Pharmacol Sci **16**, 1961–1966 (2012).

Figures

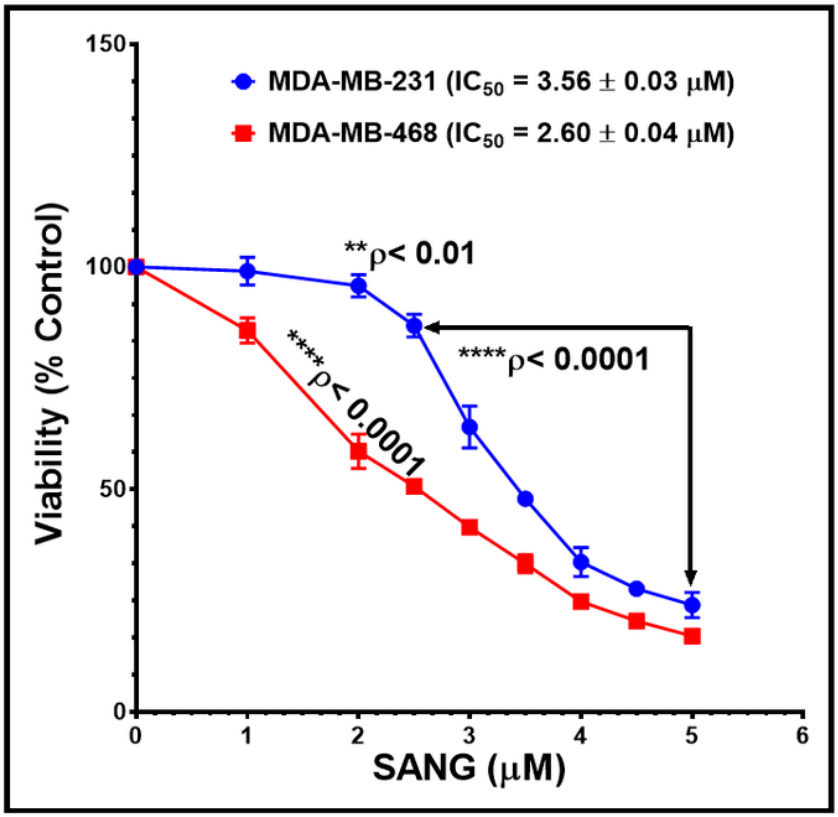

Figure 1

Cytotoxic effects of sanguinarine (SANG) in MDA-MB-231 and MDA-MB-468 cell lines. The two cell lines were seeded and treated for 24 h with 0–5 µM of SANG. The cell viability data are expressed in the graph as percentages of cell survival compared to the control. Each point represents the average ± standard error of the mean (SEM) of three biological and six technical replicates. The IC_{50} ± SEM value was averaged from the three biological replicates. The significance of the difference between the control vs. treated groups was analyzed using one-way analysis of variance (ANOVA) and was validated using Bonferroni's multiple comparisons test. The difference was considered significant at **P < 0.01 and ****P < 0.0001.

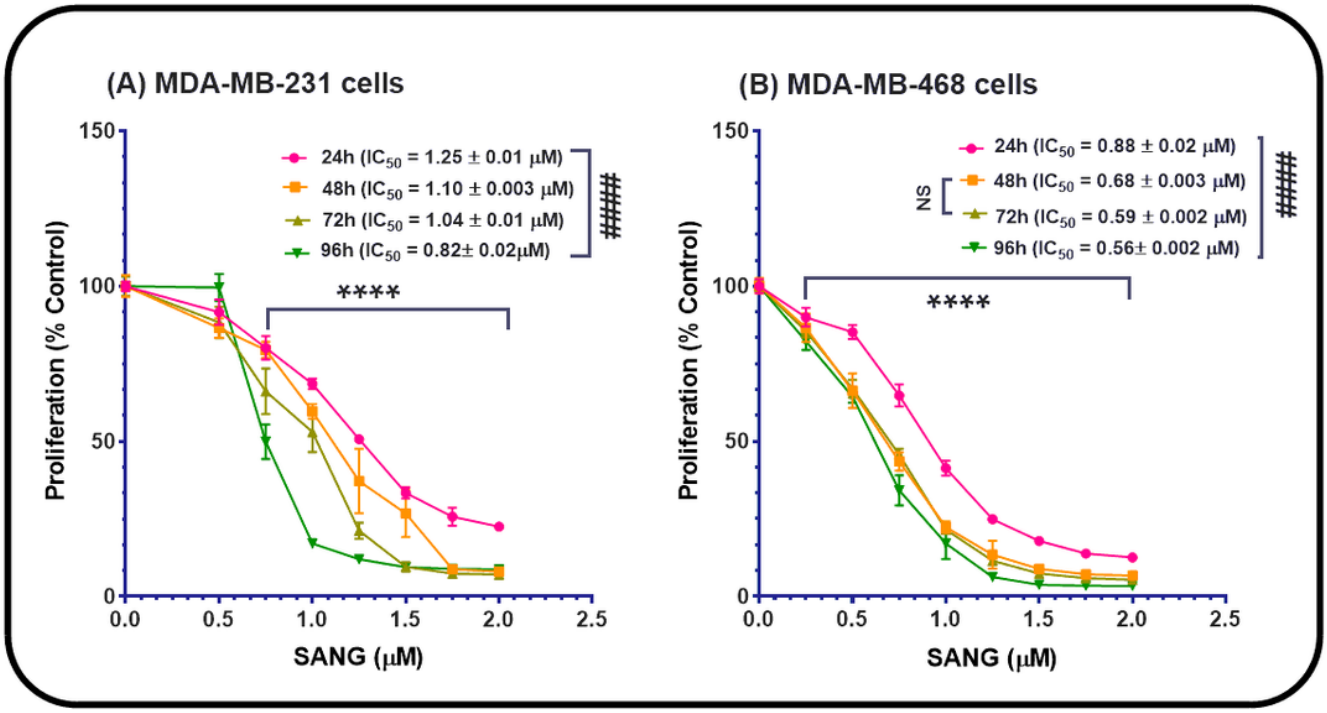

Figure 2

Effect of sanguinarine (SANG) on the proliferation rate of MDA-MB-231 and MDA-MB-468 TNBC cells. Both cell lines were consistently seeded, incubated overnight, and treated with SANG for 48–96 h with 0–2.0 μM SANG. Each data point presents the average ± SEM of three biological replicates of six technical replicates each. The IC_{50} ± SEM value was averaged from three biological replicates using excel software. ANOVA (One and Two way), followed by Bonferroni's multiple comparisons test, were used to calculate the p-values for the difference between control *vs.* treated cells at each exposure period (*) or between the different incubation periods (#), respectively. ****/#### P < 0.0001 indicates a statistically significant difference

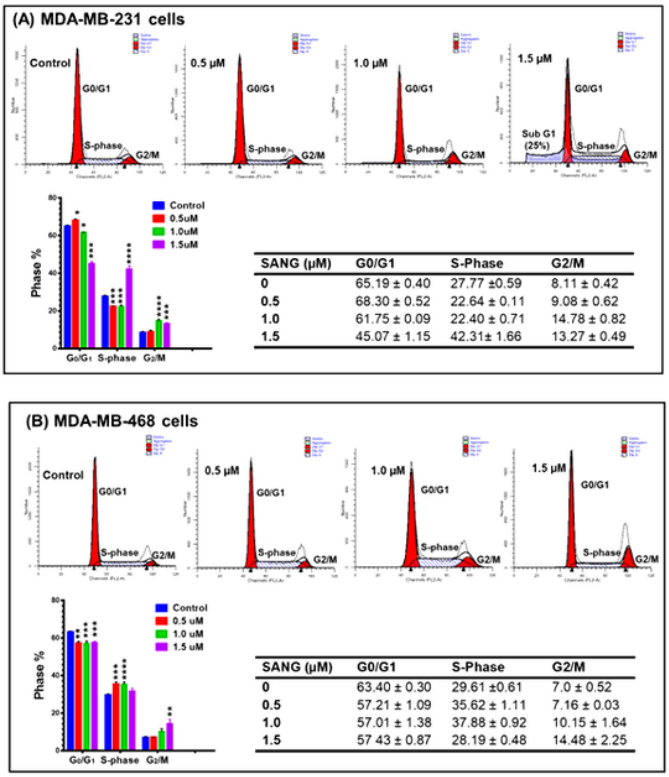

Figure 3

Effect of sanguinarine (SANG) on cell cycle progression in (a) MDA-MB-231 and (b) MDA-MB-468 TNBC cells. The growing cells were seeded and treated for 24 h with SANG at three different doses, 0–1.5 µM. Flow cytometry using the fluorescent probe PI was used to measure the changes in the DNA histogram of treated cells. For each cell line, the data were confirmed in three biological replicates with three technical replicates. FACSCalibur was used to analyze the percentage of cells in different phases among SANG-treated samples vs. control. One-way ANOVA for multiple comparisons followed by Bonferroni's test, were used to obtain the p-values. The difference between control and treated samples across the three phases was considered significant at * $P < 0.05$, ** $P < 0.01$, *** $P < 0.001$, and **** $P < 0.0001$.

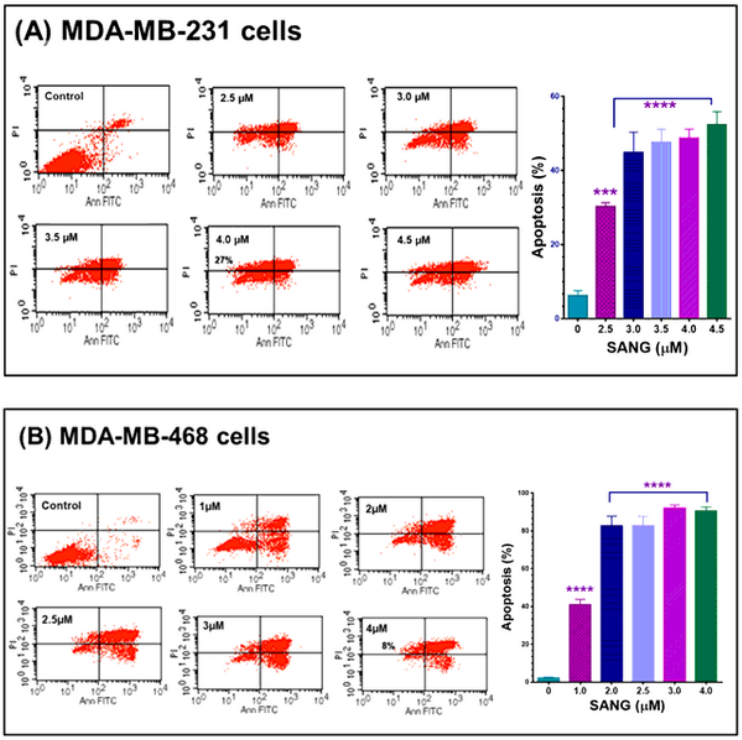

Figure 4

Apoptotic effects of sanguinarine (SANG) in (a) MDA-MB-231 and (b) MDA-MB-468 TNBC cell lines. Both cell lines were exposed to the alkaloid compound SANG for 24 h at six different concentrations ranging from 0–4.5 μM in MDA-MB-231 cells and 0–4.0 μM in MDA-MB-468 cells while control cells were exposed to < 0.1% DMSO. Both treated and control cells were labeled for 10 min with Ann FITC/PI mixture. Each bar in the graph represents the mean ± combined percentage of early and late apoptotic cells and the SEM of three biological replicates of three technical replicates. The significance of the difference between various treatments vs. control was evaluated using one-way ANOVA for multiple comparisons followed by Bonferroni's test to determine the p-values. *** $P < 0.001$ and **** $P < 0.0001$ indicate a significant difference. Ann Fitc, Annexin V-FITC; PI, propidium iodide.

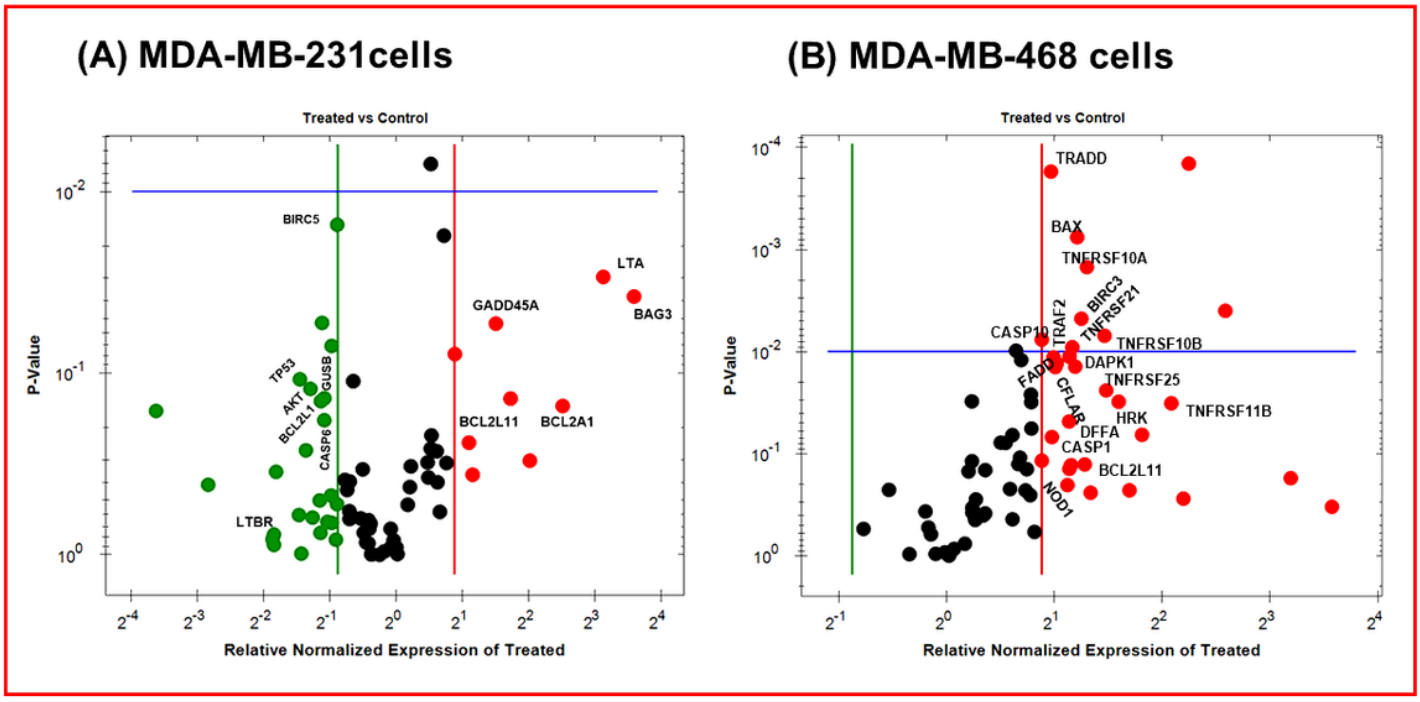

Figure 5

Categorization of apoptosis-related gene expression induced by sanguinarine (SANG) in (a) MDA-MB-231 and (b) MDA-MB-468 TNBC cells. A volcano plot illustrates the altered genes in both cell lines following 24 h exposure to the compound at 3.5 μM for MDA-MB-231 cells and 2.6 μM for MDA-MB-468 cells. The augmented mRNAs are indicated in red, and the repressed genes are indicated in green; unchanged gene expression appears as black dots. The number of upregulated genes was highly recognizable in MDA-MB-468 cells; the attenuated mRNAs were only evident in MDA-MB-231 cells.

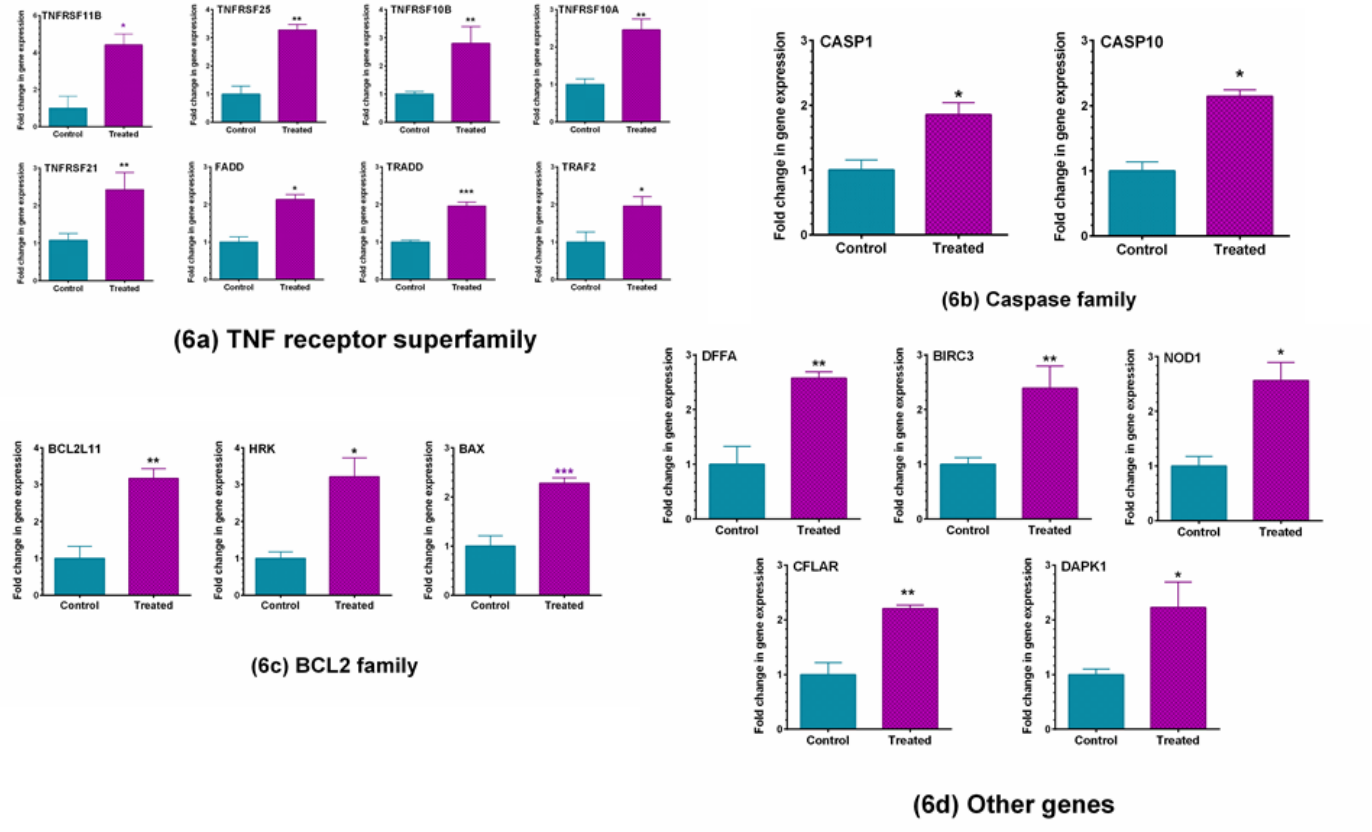

Figure 6

Gene expression quantification in sanguinarine (SANG)-treated MDA-MB-468 cells. Cells were exposed for 24 h to 2.6 μM of SANG. The transcriptomic levels of normalized mRNAs indicated a significant increase in 18 genes. (a). TNF (tumor necrosis factor) receptor superfamily (TNFRSF): 11B, 25,10B/A and 21, FAS-associated via death domain (FADD), TNFRSF1A associated via death domain (TRADD), and TNF receptor-associated factor 2 (TRAF2). (b). Caspase (CASP) 1 and 10 (c). B-cell lymphoma 2 (BCL2) like protein 11 (BCL2L11), harakiri BCL2 interacting protein (HRK), and BCL2-associated X-protein (BAX). (d). DNA fragmentation factor subunit alpha (DFFA); a baculoviral inhibitor of apoptosis (IAP) repeat-containing 3 (BIRC3); nucleotide-binding oligomerization domain-containing protein 1 (NOD1); CASP8 and FADD-like apoptosis regulator (CFLAR), and death-associated protein kinase 1 (DAPK1). The graphs represent the mean ± SEM of three biological replicates. The significance of the difference between the DMSO-treated vs. SANG-treated MDA-MB-468 cells was determined using an unpaired t-test. The difference between control and treated cells was considered significant at * $P < 0.05$, ** $P < 0.01$, and *** $P < 0.001$.

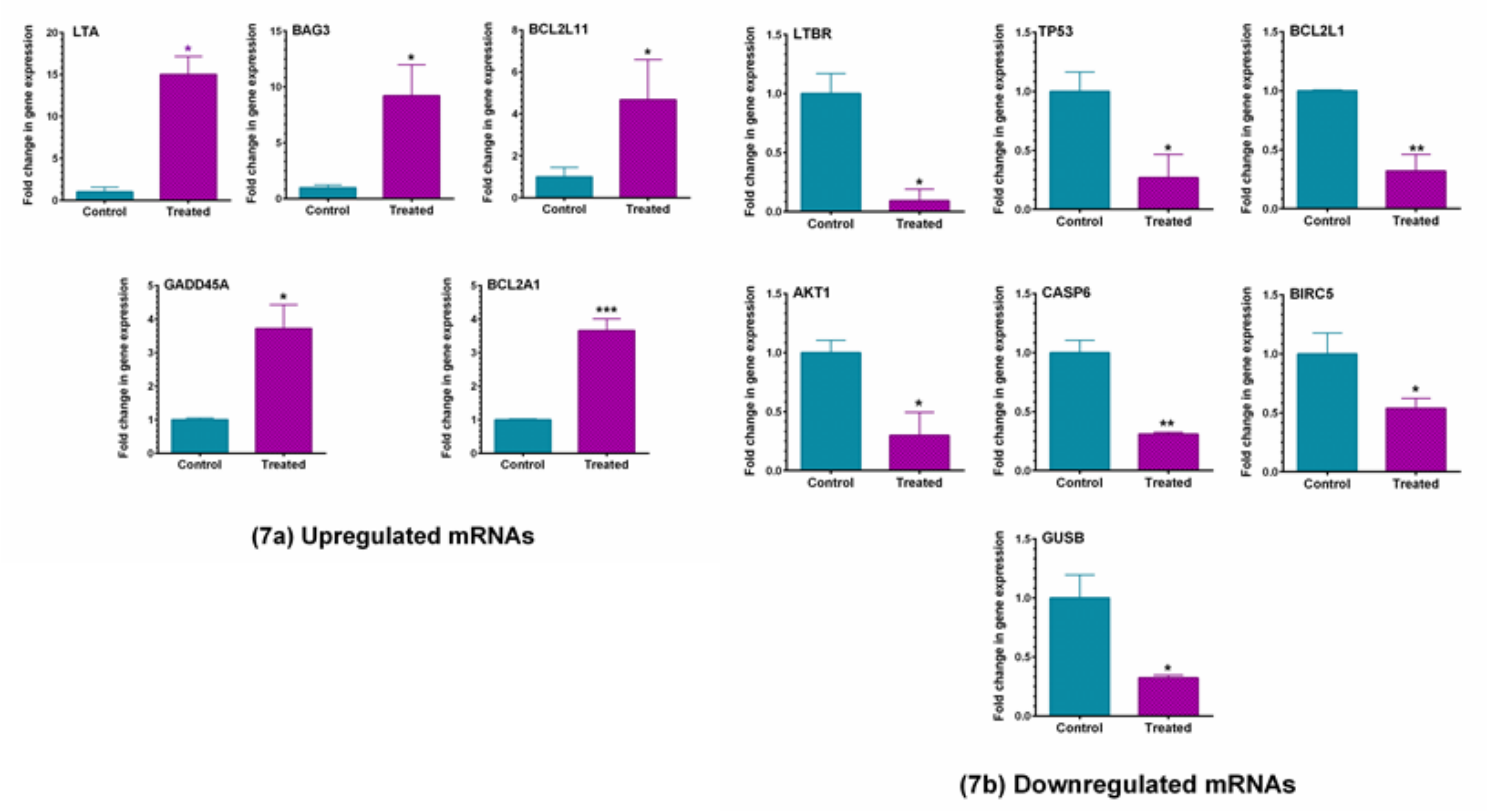

Figure 7

Gene expression quantification in sanguinarine (SANG)-treated MDA-MB-231 cells. Cells were treated for 24 h with 3.5 μM of the alkaloid compound SANG. The transcriptomic levels of normalized mRNAs indicated a significant mixed fold-change in twelve genes. (a). The upregulated mRNAs included lymphotoxin alpha (LTA), BCL2-associated athanogene 3 (BAG3), BCL2 like protein 11 (BCL2L11), the growth arrest, and DNA damage-inducible 45 alpha (GADD45A), and BCL2- related protein A1 (BCL2A1). (b). The repressed mRNAs included lymphotoxin beta receptor cells (LTBR), tumor protein p53 (TP53), BCL2 like protein 1 (BCL2L1), AKT serine/threonine kinase 1 (AKT1), CASP6, glucuronidase beta (GUSB), and baculoviral inhibitor of apoptosis family (IAP) repeat-containing 5 (BIRC5). The graphs represent the mean ± SEM of three independent biological replicates. The significance of the difference between the DMSO-treated vs. SANG-treated MDA-MB-231 cells was determined using an unpaired t-test. The difference between control and treated cells was considered significant at * $P < 0.05$, ** $P < 0.01$, and *** $P < 0.001$.

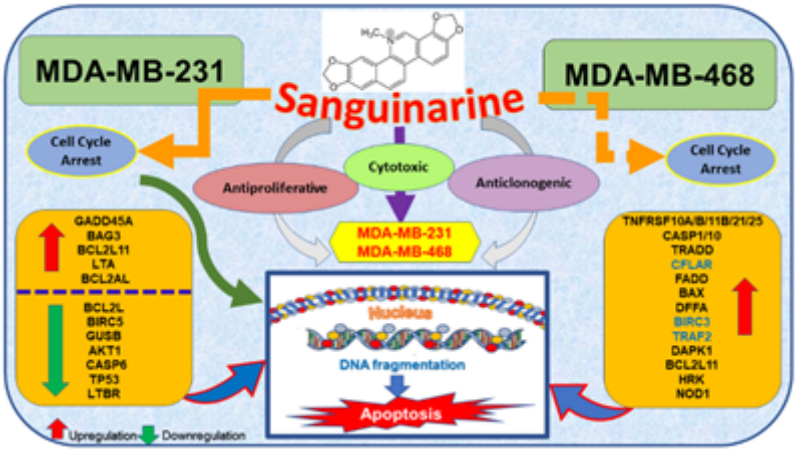

Figure 8

Schematic overview of the molecular mechanism triggering the anticancer effect of the natural alkaloid compound sanguinarine (SANG) in MDA-MB-231 and MDA-MB-468 TNBC cells.